ELSEVIER

Journal of Chromatography A, 720 (1996) 295–321

JOURNAL OF CHROMATOGRAPHY A

Review

Fluorophore-assisted carbohydrate electrophoresis in the separation, analysis, and sequencing of carbohydrates

Christopher M. Starr*, R. Irene Masada, Chuck Hague, Elisa Skop, John C. Klock

Glyko, 81 Digital Drive, Novato, CA 94949, USA

Abstract

Carbohydrate analysis has traditionally been viewed as a specialty science, performed only in a few well-established laboratories using conventional carbohydrate analysis technology (e.g. NMR, gas chromatography–mass spectroscopy, high-performance liquid chromatography, capillary electrophoresis) combined with the specialized technical training that has been essential for accurate interpretation of the data. This tradition of specialized laboratories is changing, due primarily to an increase in the number of scientists performing routine carbohydrate analysis. As a result, many scientists who are not trained in traditional carbohydrate analytical techniques now need to be able to perform accurate carbohydrate analysis in their own laboratories. This has created a need for technically simple and inexpensive methods of carbohydrate analysis. In this review, we present application vignettes of a technically simple, yet analytically powerful method called fluorophore-assisted carbohydrate electrophoresis (FACE). FACE can be used for performing routine oligosaccharide profiling, monosaccharide analysis, and sequencing of a variety of carbohydrates.

Contents

* Corresponding author.

0021-9673/96/$32.00
SSDI 0021-9673(95)00749-0

1. Introduction

The field of glycobiology is growing rapidly, primarily due to the increased awareness among scientists of the critical metabolic functions of carbohydrates in the body, as well as the importance of "correct" glycosylation in the function of recombinant glycoprotein therapeutics. The carbohydrates on glycoproteins have been shown to be important in the regulation of bioactivity [1], pharmacokinetics [2], immunogenicity [3], stability [4], and efficacy [5]. Research into the physiological roles of carbohydrates has led to a number of carbohydrate-based therapeutics, including anti-coagulants such as heparin, anti-inflammatories, selectin ligands, anti-microbials, and anti-cancer drugs. The central role played by carbohydrates in many metabolic processes helps to explain why abnormal glycosylation of cellular glycoproteins in the body often leads to disease. Carbohydrate-related diseases often result in detectable carbohydrate "markers" that can be used to diagnose specific diseases. Carbohydrate "markers" have been described for a number of human diseases including diabetes, osteoporosis, arthritis, liver disease, cancer, and a variety of inherited metabolic diseases.

This increased awareness means that scientists in both academia and industry need simple, inexpensive carbohydrate analytical methods that can be used routinely in their own laboratories and that do not require special technical training. One such method, called fluorophore-assisted carbohydrate electrophoresis (FACE) [6], has also been referred to as polyacrylamide gel electrophoresis of fluorophore-labeled saccharides (PAGEFS) [7–11]. The FACE method is based on the attachment of fluorescent dyes to the reducing end of carbohydrates followed by high-resolution separation on polyacrylamide slab gels. This review will show that the FACE method can be used to perform a wide variety of different types of analyses, on carbohydrates from many sources, including glycoproteins, glycolipids, plant and bacterial polysaccharides, as well as glycosaminoglycans (GAGs).

2. Considerations in the development of carbohydrate gel electrophoresis

2.1. Electrophoresis of carbohydrates

There are three basic problems that needed to be overcome in order to analyze carbohydrates by polyacrylamide gel electrophoresis. First, not all carbohydrates are charged, and unless they contain a charged monosaccharide (e.g. sialic acid), or are modified with $-OPO_3H^-$ or $-OSO_3^-$ groups, they will not migrate through a gel by electrophoresis. In fact, the only general types of carbohydrates routinely analyzed by polyacrylamide gel electrophoresis have been the charged glycosaminoglycans [12–14]. This charge requirement for FACE analysis led to a family of negatively charged fluorescent tags including ANTS, ANDA, and ANSA, shown in Fig. 1. Once a carbohydrate is derivatized with one of these charged fluorescent tags, the carbohydrate molecule will possess an overall net negative charge, regardless of the charge status of the native carbohydrate molecule, and therefore will migrate in an electric field. This illustrates an

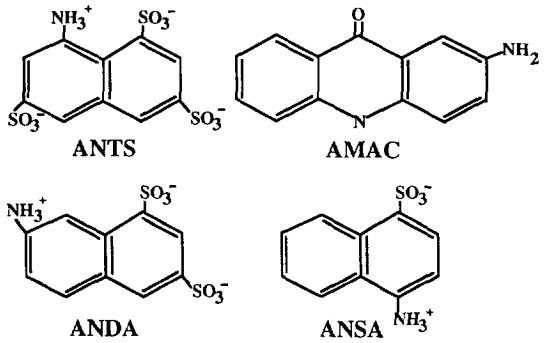

Fig. 1. Fluorophores used in FACE. Shown are the structures of four fluorophores used in FACE: disodium 8-amino-naphthalene-1,3,6-trisulfonate (ANTS), 2-aminoacridone (AMAC), potassium 7-amino-1,3-naphthalene disulfonate (ANDA) and sodium 4-amino-naphthalene sulfonate (ANSA). In general, the charged fluorophores ANTS, ANDA, and ANSA are used for oligosaccharide profiling applications and AMAC is used for monosaccharide compositional analysis.

important attribute of derivatization in carbohydrate analysis, which is, that by changing the nature of the fluorescent tag, the chemical or charge properties of the derivatized carbohydrate molecule can be modified to suit a particular application. As we will show, different fluorescent tags can be used to alter the mobility of monosaccharides and oligosaccharides in a gel so as to achieve optimal separations for specific applications.

2.2. Detection of carbohydrates on gels

The second problem encountered in the electrophoresis of carbohydrates is the requirement for accurate carbohydrate quantification. This means that both the labeling and the detection system employed must be quantitative. Electrophoresis of proteins and DNA on slab gels often involves the use of, at best, semi-quantitative stains, for example, Coomassie Blue for proteins and ethidium bromide for DNA. A good general stain that can be used to detect a wide variety of carbohydrates on gels has not been found. Many methods of carbohydrate analysis use radiolabeling with tritiated sodium borohydride as a means of detection and quantification [15], but problems related to radioisotope containment and disposal of large volumes of liquid waste, limits the routine use of long half-life radioisotopes in electrophoresis. Also, the low-level beta radiation from tritium will not escape the environment of a wet gel. Therefore, the gel would need to be soaked in a scintillant prior to autoradiography, which leads to significant diffusion of the carbohydrates bands in the gel. The fluorescent tags used in FACE offer a high level of detection sensitivity, rivaling that of radiolabeling, even in a wet gel environment, without the need for radioisotope containment.

2.3. Principles of electrophoretic separations of carbohydrates

The third problem encountered with separating carbohydrates by gel electrophoresis is that oligosaccharides are relatively small molecules relative to the pore size of the gel matrix. Whereas the molecular masses of proteins and DNA usually range in the 10 000s, N-linked-type oligosaccharides are generally in the range of a few 1000 and monosaccharides in the range 180–300. Therefore, in order to separate oligosaccharides, very high percentage polyacrylamide gels must be employed. We routinely use gels containing 20–40% T acrylamide, but these gels are very difficult to cast and have a shelf stability of only a few hours. Because consistent gel quality is essential for comparing electrophoresis patterns from different experiments, we use a temperature-controlled gel casting procedure and vacuum-packed storage conditions that allow multi-casting of 10×10 cm polyacrylamide gels with 4–12 month shelf storage depending on the percentage of acrylamide.

Separation of oligosaccharides on polyacrylamide gels is influenced by both their intrinsic charge (i.e. contributed by sialic acid, $-OPO_3H^-$, $-SO_3^-$, etc.) and by their size or hydrodynamic volume. As shown in Fig. 2, relatively large oligosaccharides that contain sialic acid (e.g. the trisialylated, triantennary oligosaccharide in lane 5) migrate faster than smaller neutral oligosaccharides (e.g. $Man_9GlcNAc_2$ in lane 3). This is because the carboxyl groups on the sialic acid residues in-

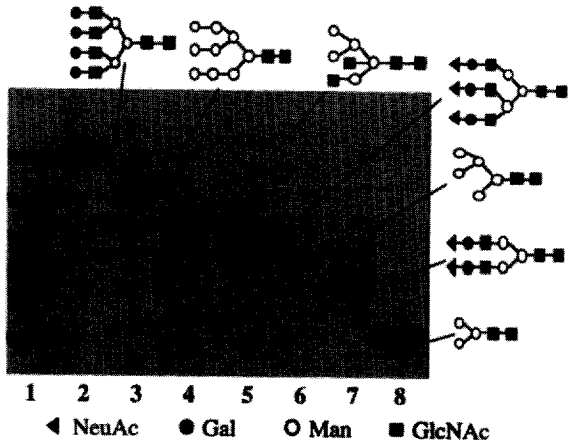

Fig. 2. Principles of FACE oligosaccharide separations. Profiles of various types of ANTS-labelled N-linked oligosaccharide standards (Dionex, CA, USA) are shown. Lane 1 contains a mixture of oligosaccharides in lanes 2–8. Lanes 2–8 contain the oligosaccharides whose structures are shown in the figure. This profile illustrates the effects of charge and size on oligosaccharide mobility. Each lane contains 50 pmol of oligosaccharide.

crease the net negative charge on the larger oligosaccharide, causing it to migrate faster on the gel. When analyzing neutral oligosaccharides, the separation is based on the hydrodynamic size of the oligosaccharide with the smaller oligosaccharide, $Man_3GlcNAc_2$, shown in lane 8, running farther down in the gel than the $Man_5GlcNAc_2$, in lane 6, which in turn runs faster than the $Man_9GlcNAc_2$ in lane 3. These observations explain why the migration of large oligosaccharides that contain sialic acid is shifted to higher positions on the gel following the removal of the sialic acid residues with neuraminidase (Figs. 4, 12 and 13). The migration pattern of different oligosaccharides is highly reproducible [16] and the DP positions of various N-linked-type oligosaccharides relative to a standard ladder of glucose polymers are shown in Table 1.

3. FACE labeling chemistry and reaction kinetics

FACE involves labeling the carbohydrate by reductive amination. The primary amine of a fluorescent tag and the C-1 aldehyde of the reducing sugar react to form a Schiff base, which is reduced to the mixed aryl/aliphatic secondary amine by sodium cyanoborohydride, as shown in Fig. 3A. Step I indicates the equilibrium that exists between the hemi-acetal and the aldehyde of the reducing sugar which occurs spontaneously whenever the sugar is in solution. The addition of the tag to the reducing end of the carbohydrate forms through a fast equilibrium between the aldehyde and the Schiff base (Step II, Fig. 3A). Formation of the Schiff base is kinetically rapid, but thermodynamically unfavorable [17]. Therefore, continuous reduction of the rapidly forming Schiff base by $NaBH_3CN$ forces the reaction to completion in the formation of the stable amine (Step III, Fig. 3A). This reduction step is probably the overall rate-limiting step of the labeling reaction [18].

An important consideration about any labeling procedure is the efficiency and specificity of the derivatization step. To address this concern, experiments were performed to determine the labeling kinetics of chitotriose; a molecule that contains three beta-linked GlcNAc residues, and therefore contains the same monosaccharide composition and linkage as the reducing end of an N-linked-type oligosaccharide. Experiments were performed using increasing labeling times (Fig. 3B) and increasing amounts of chitotriose (Fig. 3C). In all these experiments, quantification of the chitotriose band was determined against a standard of fluorophore-labeled glucose which has been shown to label to >95% at 37°C for 15 h using our standard labeling conditions [19]. When labeling relatively small amounts of sugar, fluorophore labeling by reductive amination is very efficient, with >80% of the oligosaccharides labeled in 6 h, and >95% labeled after 16 h (Fig. 3B). However, if the total amount of oligosaccharide in the labeling reaction is >25 nmol, labeling efficiency may decline (Fig. 2C). These results may help explain the reports of low labeling efficiency using reductive amination by alternative carbohydrate analytical techniques that require the labeling of nanomole or even micromole amounts of carbohydrate for detection.

The FACE method allows for the high sen-

Table 1
DP position of ANTS-labeled N-linked oligosaccharides

Type	Description	DP
Complex	1. disialylated, galactosylated biantennary (2 α2–6)	5.4 ± 0.3
	2. disialylated, galactosylated biantennary, core-fucosylated (2 α2–6)	5.7 ± 0.2
	3. disialylated, galactosylated biantennary, core-fucosylated (2 α2–3)[a]	6.2[b]
	4. trisialylated, galactosylated triantennary (2 α2–6)	6.2 ± 0.3
	5. trisialylated, galactosylated triantennary (2 α2–3)	6.7 ± 0.4
	6. trisialylated, galactosylated triantennary, core-fucosylated (3 α2–3)[b]	7.0[b]
	7. tetrasialylated, galactosylated tetraantennary (isomers)	7.6[b],7.2[b],6.7[b],6.2[b]
	8. asialo-, galactosylated biantennary	7.8 ± 0.2
	9. asialo-, galactosylated biantennary, core-fucosylated	8.5 ± 0.3
	10. asialo-, galactosylated biantennary, bisecting GlcNAc, core-fucosylated	8.5 ± 0.3
	11. asialo-, galactosylated triantennary	9.6 ± 0.3
	12. asialo-, galactosylated triantennary, core-fucosylated[a]	10.5 ± 0.5
	13. asialo-, galactosylated tetraantennary	11.5 ± 0.4
	14. asialo-, galactosylated tetraantennary, core-fucosylated[a]	12.1 ± 0.1
	15. asialo-, agalacto-, biantennary	5.6 ± 0.5
	16. asialo-, agalacto-, biantennary, core-fucosylated	6.2 ± 0.2
	17. asialo-, agalacto-, triantennary	6.4 ± 0.4
	18. asialo-, agalacto-, triantennary, core-fucosylated[a]	7.1[b]
	19. asialo-, agalacto-, tetraantennary	7.3 ± 0.3
	20. asialo-, agalacto-, tetraantennary, core-fucosylated[a]	7.9[b]
Hybrid	21. hybrid type with bisecting GlcNAc	7.0 ± 0.3
High-mannose	22. oligomannose 9	8.8 ± 0.3
	23. oligomannose 8	8.1 ± 0.2
	24. oligomannose 7	7.4 ± 0.4
	25. oligomannose 6	6.5 ± 0.2
	26. oligomannose 5	5.7 ± 0.3
Core	27. conserved trimannosyl core	4.2 ± 0.2
	28. conserved triamannosyl core, core-fucosylated	4.8 ± 0.1
	29. Man(α1,6/3)Man(β1,4)GlcNAc(β1,4)GlcNAc[a]	3.3 ± 0.1
	30. Man(α1,6/3)Man(β1,4)GlcNAc(β1,4)[Fuc(α1,6)]GlcNAc[a]	4.0[b]
	31. Man(β1,4)GlcNAc(β1,4)GlcNAc	2.5 ± 0.1
	32. Man(β1,4)GlcNAc(β1,4)[Fuc(α1,6)]GlcNAc	3.2 ± 0.2

[a] Sequence determined by FACE, some undetermined linkages.
[b] DP average from less than six values.
This table lists the DP (degree of polymerization) positions of standard N-linked oligosaccharides (Dionex, CA, USA) relative to the glucose polymer ladder standard using the Glyko imaging system. The DP numbers shown represent the average ± range of six independent determinations for each oligosaccharide.

sitivity of fluorescence with detection limits into the low picomole range. This means that the amount of carbohydrate that needs to be labeled in each reaction can be maintained within the low nanomole range. The high labeling efficiency achieved in FACE may also result from the use of $NaBH_3CN$ as the reducing agent instead of $NaBH_4$. During the labeling process the reducing agent ($NaBH_3CN$ in FACE) and the primary amine on the tag are essentially competing with each other for reaction with the C-1 aldehyde group of the pyranose form of the reducing sugar (step II in Fig. 3A). $NaBH_3CN$ is much less active toward the C-1 aldehyde than $NaBH_4$, meaning that less of the sugar will be reduced directly to the alcohol and more of the sugar will remain in the unreduced form available for labeling [20].

Some labeling procedures that use reductive amination have been reported to show oligosaccharide selectivity which may lead to inaccurate quantification of oligosaccharides with dif-

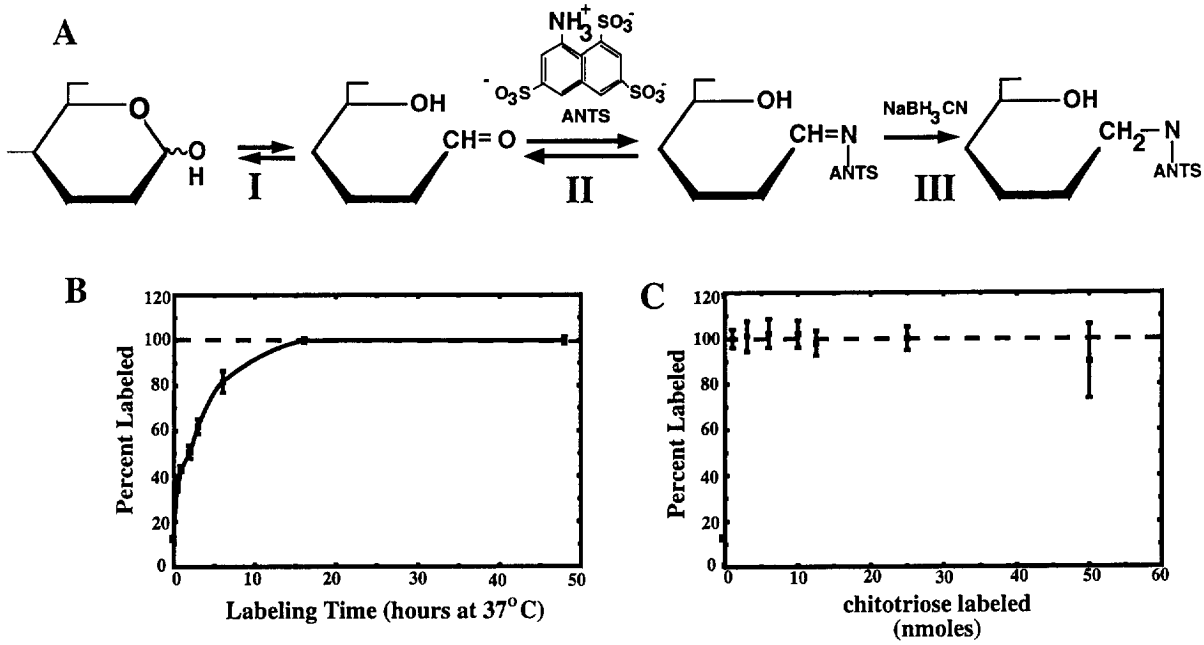

Fig. 3. FACE labeling chemistry. (A) The fluorophore labeling reaction with ANTS forming the Schiff base and reduction by $NaBH_3CN$. (B) The labelling kinetics of 2 nmol of chitotriose using 5 μl of 0.15 *M* ANTS and 5 μl of 1.0 *M* $NaBH_3CN$ at 37°C. (C) The percent labeling efficiency of increasing amounts of chitotriose with the same concentrations of ANTS and $NaBH_3CN$ for 16 h. At least 25 nmol of chitotriose can be labeled without a decrease in efficiency.

ferent structures [21]. Because in many situations the same monosaccharide is actually being labeled (e.g. all N-linked oligosaccharides contain GlcNAc at the reducing end), we believe that this reported selectivity may actually be related to degradation of the oligosaccharide (loss of sialic acid primarily) during labeling. Indeed, degradation of some oligosaccharides will occur during labeling if the labeling temperature is permitted to exceed 50°C. However, we have not detected oligosaccharide degradation of even sialic acid containing oligosaccharides when labeling is performed at 37°C.

The possibility that selective labeling might occur led us to perform the following experiments. Using a number of commercially available oligosaccharide standards (Dionex, CA, USA; Oxford Glycosystems, UK; and Accurate Chemicals, NY, USA), we found that the labeling of different oligosaccharides either individually or in mixtures was essentially equivalent (data not shown). Because quantitative standards are not available for N-linked oligosaccharides, we also performed a series of experiments to generate equivalent amounts of oligosaccharides with different structures. We took a standard oligosaccharide structure (the example shown in Fig. 4 uses a standard trisialylated, triantennary oligosaccharide, as determined by NMR and HPLC, from Dionex, CA, USA), aliquoted equal amounts (50 pmol) into five tubes and digested each with different combinations of glycosidases using the sequencing strategy shown in Fig. 4. This created a set of five oligosaccharides, of equal amounts, but with different sugars at their non-reducing terminus, as shown along the right side of the gel in Fig. 4. For example, according to the scheme in Fig. 4, the first reaction contained no enzyme (lane 2) and is designated the starting material. The second contained neuraminidase alone (lane 3), which resulted in a galactose terminating triantennary oligosaccharide with all sialic acids removed by the enzyme. The third reaction (lane 4) contained both neuraminidase and β-galactosidase, resulting in GlcNAc terminating oligosaccha-

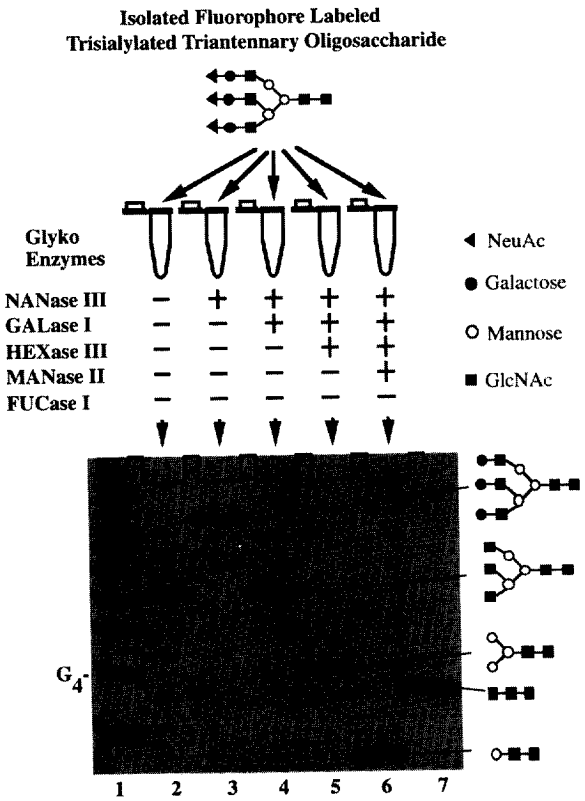

Fig. 4. Uniformity of FACE labeling chemistry. The labeling efficiency of a variety of complex types of N-linked oligosaccharides with different structures. Equimolar amounts of a trisialylated triantennary oligosaccharide standard (Dionex FT07) were digested with exo-glycosidases prior to fluorophore labeling to produce a variety of different complex type oligosaccharides. The various oligosaccharides were then labeled with ANTS, profiled, and the oligosaccharides quantified. The digestions, labeling, and profiling were done in triplicate and each oligosaccharide was quantified to within 12% C.V. of each other. This figure illustrates the sequence strategy of ANTS-labeled isolated N-linked-type oligosaccharides. Lane 1 contains the OLIGO Ladder Standard, which is a mixture of glucose polymers, and the maltotetraose band (G4) contains 50 pmol. Lane 2 contains the undigested oligosaccharide; lane 3, the neuraminidase (α2–3,6,8) digested oligosaccharide; lane 4, the neuraminidase and β-galactosidase (β1–3,4,6) digested oligosaccharide; lane 5, the neuraminidase, β-galactosidase, and β-N-acetylhexosaminidase (β1–2,3,4,6) digested oligosaccharide; lane 6, the neuraminidase, β-galactosidase, β-N-acetylhexosaminidase and α-mannosidase (α1–2,3,6) digested oligosaccharide; lane 7 contains 50 pmol of chitotriose.

rides. Similar reactions were performed on the other aliquots as described in the legend to Fig. 4, with one additional enzyme added to each so that the last tube contained all the enzymes required to degrade the oligosaccharide to the mannosylchitobiose core ($ManGlcNAc_2$). Following the reactions, all the digests were labeled with ANTS and separated on a polyacrylamide gel, an image of which is shown in Fig. 4. This experiment resulted in a series of oligosaccharides, all of equal amounts (we started with equal aliquots), but containing oligosaccharides with different monosaccharide compositions and structures. When the data from triplicate experiments were analyzed and the quantification of the five different structures were combined, we calculated a percent coefficient of variation (%C.V. = S.D./mean × 100) of less than 12%. We have seen a reduction in efficiency and perhaps some selectivity occurring when more than 25 nmol total oligosaccharide was labeled in one reaction. Therefore, we routinely limit our labeling reactions to less than 20 nmol for accurate band quantification. Fortunately, the sensitivity of fluorescence detection is such that labeling >20 nmol is usually not required for analytical work.

4. Gel imaging and carbohydrate analysis

Accurate quantification is essential for detailed carbohydrate analysis. Although the oligosaccharide patterns on FACE gels can be viewed and photographed on a standard laboratory UV light box, photographic film is not reliable for accurate quantification. To visualize the carbohydrate banding patterns, the gel, still within the glass cassette, is placed on a long-wave UV lightbox (e.g. UVP, Cambridge, UK, Model TL-33 or equivalent) with a peak excitation output at approximately 360 nm. To photograph the banding pattern, a medium speed, medium resolution Polaroid film is used. The camera should be equipped with an appropriate emission filter, for example, a Kodak Wratten No. 8 or equivalent (i.e. peak transmission at approximately 500 nm and bandwidth of 80 nm). Exposure times of 1–2

min are generally required. The quantitative data presented in this review were obtained by imaging the gels following electrophoresis using a CCD (charge-coupled device)-based imaging system (Glyko). Following electrophoresis, the gel was inserted into the imager under long-wavelength UV excitation, and an electronic image of the fluorescent carbohydrate banding pattern of the gel was acquired by the imager's CCD as a digital image [22,23]. The gel image was displayed on a computer screen using FACE Imaging Software through an MS-Windows interface. This imaging system allows for detection and quantification of individual carbohydrate bands into the low picomole range of 1.6 to 300 pmol, as shown in Fig. 5A. A linear plot of the actual picomoles loaded onto the gel versus the picomoles measured by the imager is shown in

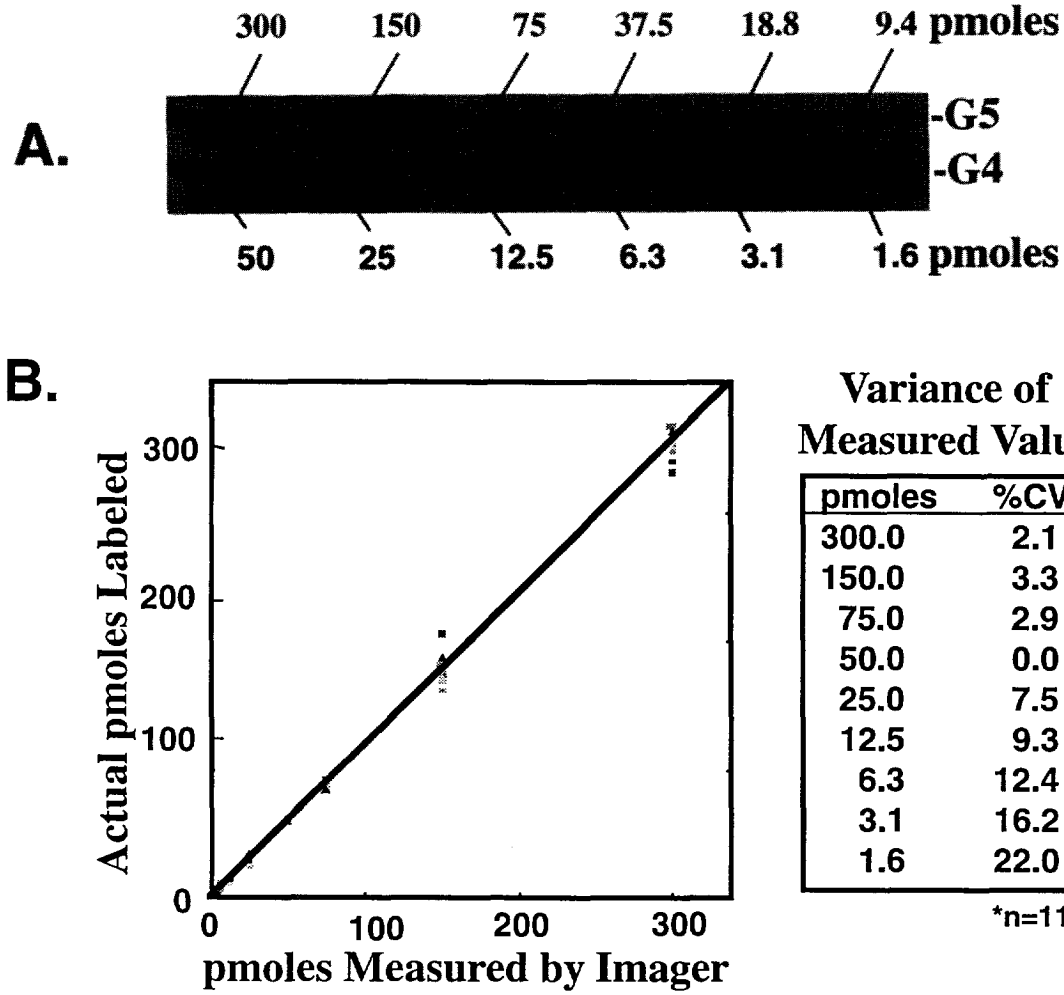

Fig. 5. FACE gel imaging and quantification. (A) One of eleven profiling gels that were prepared to determine the dynamic range and sensitivity of the FACE imager. Each gel has bands containing from 300 to 9.4 pmol of ANTS-labeled maltopentaose (top row) and 50 to 1.6 pmol of ANTS-labeled maltotetraose (bottom row). The 50-pmol band in each gel was used as an internal quantification standard and recorded as 50 pmol. (B) The pmol quantity determined by the imager from each of the eleven gels plotted against the actual number of pmol labeled. The equation of the best-fit line through these points shows a slope of 1.01, with a correlation coefficient $r^2 = 0.997$. The percent coefficient of variation (%C.V. = S.D./mean × 100) for each quantity level is shown on the right.

Fig. 5B. A statistical analysis of the point spread from eleven duplicate gels at each picomole level is shown on the right. The percent coefficient of variation (%C.V. = S.D./mean × 100) is less than 10% for all band quantities above 6 pmol and below 5% for band quantities above 50 pmol. The imager was able to detect bands as low as 1.0 pmol, but the %C.V. was greater than 20% at and below this level. In practice, the most useful and accurate range of the imager for band quantification is between 5 and 500 pmol of carbohydrate and this range was used for the experiments described in this paper.

5. Glycoconjugate-derived oligosaccharide profiling

The first step in the profiling of oligosaccharides attached to glycoconjugates is the release of the intact oligosaccharides. As the mechanisms and techniques for the release of oligosaccharides are discussed elsewhere in this volume, the release step will not be dealt with here except to say that in order to perform subsequent FACE analysis, the release step must not result in the reduction of the carbohydrate molecule. That is, the terminal sugar of the oligosaccharide must remain in the non-reduced form for labeling. Release of N-linked oligosaccharides from glycoproteins is routinely performed using the recombinant form of the glycoamidase, peptide-N-glycosidase F, as detailed below [24]. This enzyme non-specifically releases all types of asparagine-linked (N-linked) oligosaccharides. For more selective release of different types of N-linked oligosaccharides, a variety of endoglycosidases can be used, including endo N-acetylglucosaminidase H (Endo H), as well as the endoglycosidases isolated from *Flavobacteria* (Endo F1, F2, F3) [25]. Unfortunately, non-selective enzymes have not been found for the release of O-linked oligosaccharides (O-glycosidase only releases unsubstituted, ser/thr Galβ1-3GalNAc), so chemical release mechanisms must be used. For release of O-linked oligosaccharides from serine or threonine, we perform hydrazinolysis, using anhydrous hydrazine. Hydrazine non-selectively releases O-linked oligosaccharides with good release efficiency (>75%), and if performed with care, does not result in significant oligosaccharide degradation [26]. Finally, the release of oligosaccharides from glycosphingolipids is accomplished using ceramide glycanase. We use the enzyme isolated from the leech species *Marobdella decora*, which, in the presence of the detergent sodium cholate, results in 65–75% release of the oligosaccharides from the ceramide [27].

5.1. FACE profiling of glycoprotein-derived oligosaccharides

The FACE pattern of N-linked oligosaccharides released from a number of different glycoproteins is shown in Fig. 6. The FACE N-linked oligosaccharide profiling procedure began with

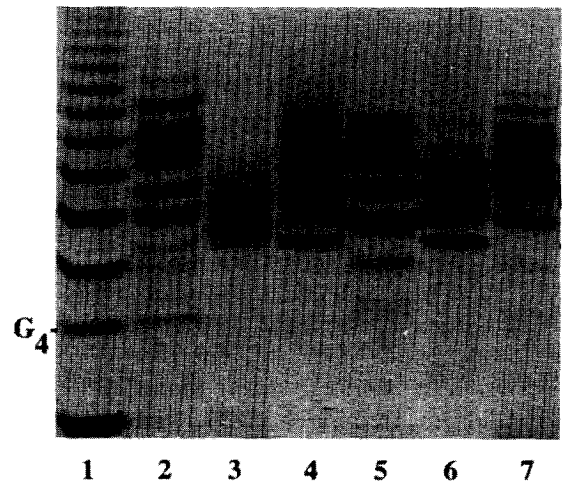

Fig. 6. FACE glycoprotein-derived oligosaccharide profiling. Profiles of ANTS-labeled oligosaccharides released by peptide-N-glycosidase (PNGase F) from six different glycoproteins are shown. Lane 1 contains the OLIGO Ladder Standard; lane 2, chicken trypsin inhibitor; lane 3, bovine fetuin; lane 4, human α_1-acid glycoprotein; lane 5, bovine ribonuclease B; lane 6, human chorionic gonadotropin (hCG); and lane 7, chicken ovalbumin. The profiles show a wide variety of different glycosylation patterns, indicating the minimum number (some oligosaccharides will co-migrate) of different types of oligosaccharides present and their relative quantities.

denaturing the glycoprotein in 50 μl of 50 m*M* phosphate buffer, pH 7.5, containing 0.1% sodium dodecyl sulfate (SDS), heating at 100°C for 5 min, then adding 5 μl of 7.5% NP-40. Oligosaccharides were then released using 5 mU of recombinant peptide-N-glycosidase F (rPNGase F, Glyko). The reaction was incubated for 2 h at 37°C. The deglycosylated protein was precipitated by the addition of 3 volumes of cold 100% ethanol, and the released oligosaccharides were recovered in the ethanol supernatant following centrifugation. The ethanol supernatants containing the released oligosaccharides from each of the digests were dried in a centrifugal vacuum evaporator (CVE) and labeled by the addition of 5 μl of the fluorescent dye 0.15 *M* ANTS (disodium 8-aminonaphthalene-1,3,6-trisulfonate) in 15% acetic acid and 5 μl of 1.0 *M* $NaBH_3CN$ in dimethylsulfoxide (DMSO). The labeling reaction was incubated overnight (16 h) at 37°C and then dried in a CVE. The labeled oligosaccharides were resuspended in 12.5% glycerol containing a Thorin dye marker. Oligosaccharide separations were performed on precast oligosaccharide profiling gels (Glyko) containing 21% polyacrylamide at a constant current of 20 mA at 5°C for 1 h.

The glycoproteins in Fig. 6 each show a different oligosaccharide pattern due to differences in oligosaccharide composition. For example, Fig. 6, lane 5 shows the size-based separation of neutral oligomannose oligosaccharides released from ribonuclease B; $Man_5GlcNAc_2$ is the lowest major band (a faint $Man_4GlcNAc_2$ band is also visible), with $Man_5GlcNAc_2$ – $Man_9GlcNAc_2$ forming the ladder. Lane 3 shows the separation of complex, charged oligosaccharides released from fetuin. The upper band is actually a doublet located at approximately DP = 6.2 and 6.5, which contains the trisialylated, triantennary oligosaccharides of fetuin. The upper oligosaccharide of the doublet contains two α2–3 linked sialic acid residues and one α2–6 linked sialic acid, and the lower band contains one α2–3 linked sialic acid and two α2–6 linked sialic acids. This illustrates that FACE profiling is sensitive to relatively small structural features that affect the hydrodynamic volume of the oligosaccharides, and that these structural features result in discernible differences in oligosaccharide mobility. The lower doublet bands at DP = 5.2 and 5.55 also contain triantennary, but with an additional sialic acid attached α2–3 to GlcNAc on one of the branches. As you might expect, small changes in the percentage of polyacrylamide in the gel can greatly influence the resolving power of the gel [28]. The ability to detect mobility shifts in FACE gels has been used to determine lectin binding kinetics [29], protein binding to glycosaminoglycans [30], and is fundamental to the FACE sequencing strategy described below. In this profiling gel the G4 band in lane 1 contains 50 pmol of maltotetraose. The faintest bands in the oligosaccharide profiles shown in Fig. 6 contain 5–10 pmol of carbohydrate.

5.2. FACE profiling of oligosaccharides released from glycosphingolipids

The FACE profile of oligosaccharides released from purified brain glycosphingolipids is shown in Fig. 7. The oligosaccharides were released from 10 μg of each glycosphingolipid using 50 mU ceramide glycanase (Glyko) in 1.8 m*M* sodium cholate and 50 m*M* phosphate buffer at pH 5.0. The reaction was mixed and incubated overnight (16 h) at 37°C. Following the incubation, the reaction was extracted with 250 μl of chloroform–methanol (2:1, v/v), centrifuged for 5 min, and the aqueous phase (upper layer) was recovered and dried in a CVE. The released oligosaccharides were labeled by the addition of 5 μl of the fluorescent dye 0.15 *M* ANDA (potassium 7-aminonaphthalene-1,3-disulfonate) in 15% acetic acid and 5 μl of 1.0 *M* $NaBH_3CN$ in DMSO. The labeling reactions were dried in a CVE, resuspended in 20 μl water, and 2 μl was combined with 2 μl of 12.5% glycerol containing a Thorin dye marker. Oligosaccharide separations were performed on precast profiling gels containing 21% polyacrylamide (Glyko) at a constant current of 20 mA at 5°C for 1 h.

The oligosaccharides from glycosphingolipids are often smaller than N-linked oligosaccharides released from glycoproteins, and may have a

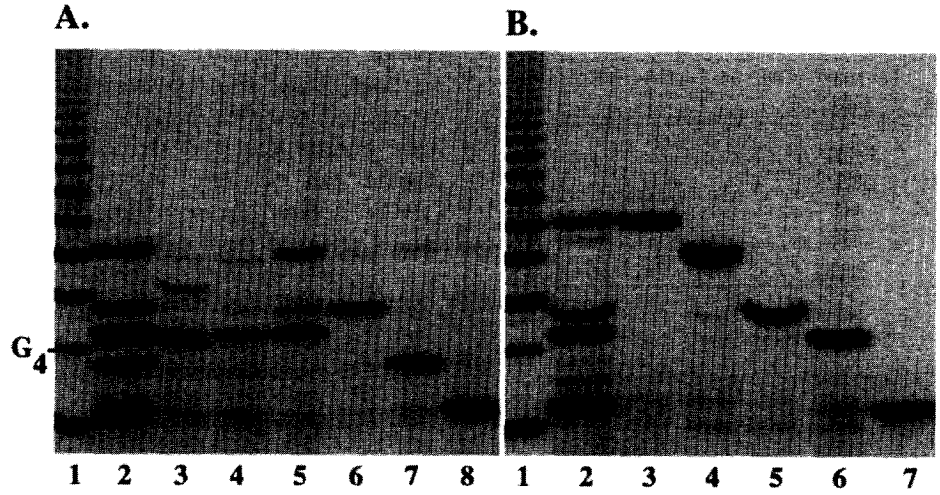

Fig. 7. Glycosphingolipid-derived oligosaccharide profiling. Profiles of ANDA-labeled oligosaccharides released by leech, *Marobdella decora*, ceramide glycanase from acidic and neutral sphingolipids (gangliosides) are shown. Lane 1 in both images contains the ANTS-labeled OLIGO Ladder Standard. In (A), lane 2 contains a mixture of the ANDA-labeled oligosaccharides from acidic sphingolipids plus asialo GM_1 (slowest mobility); lane 3, from GT_{1b}; lane 4, from GD_{1a}; lane 5, from GD_{1b}; lane 6, from GM_1; lane 7, from GM_2; and lane 8, from GM_3. In (B), lane 2 contains a mixture of ANDA-labeled oligosaccharides from neutral sphingolipids; lane 3, from LNF I-ceramide; lane 4, from Forssman glycolipid; lane 5, from Gb_4; lane 6, from Gb_3; and lane 7 contains ANDA-labeled lactose.

higher charge density. Therefore, we often get better resolution during profiling using ANDA, a fluorescent tag with less negative charge than ANTS (see Fig. 1 for fluorophore structures). The profiles shown in Fig. 7 were labeled using ANDA, which can be used to separate most acidic and neutral glycosphingolipid-derived oligosaccharides. ANTS can also be used to label oligosaccharides released from glycosphingolipids [31], and can be used as an alternative fluorophore if the ANDA-labeled oligosaccharides are suspected to co-migrate on the gel. Because specific glycosphingolipid-derived oligosaccharides that co-migrate using ANTS can often be resolved using ANDA, and vice versa, we routinely analyze glycosphingolipid unknowns using both ANTS and ANDA.

5.3. FACE profiling of glycosaminoglycans

The mucopolysaccharidoses (MPS) are a group of lysosomal storage diseases that are caused by deficiencies in the lysosomal glycosidases which degrade GAGs in the cell. Different MPS diseases are characterized by the excretion of specific GAGs into the urine [32–35]. To illustrate the use of FACE for the analysis of GAGs, Fig. 8 shows a profile of the urinary GAGs excreted by patients with mucopolysaccharidoses. For the analysis, the urinary GAGs were precipitated from the urine of patients by adding 0.5 ml of CPC (cetylpyridinium chloride) reagent (0.2 *M* sodium citrate, 0.1% CPC, pH 4.8) and incubating for 30 min at 37°C. The CPC precipitate was recovered by centrifuging for 5 min at 14 000 *g*, and discarding the supernatant. The CPC pellet was washed by dissolving the pellet in 67 μl 2 *M* LiCl, adding 267 μl cold, 100% ethanol, and re-precipitating the pellet for 2 h at 4°C. The washed CPC pellet was recovered by centrifuging for 5 min at 14 000 *g* and re-suspending the pellet in 50 μl of water. Then 30 μl was removed for monosaccharide composition analysis (described below), and 20 μl was labeled with ANTS as described for glycoprotein oligosaccharide profiling. The labeled carbohydrates were dried in a CVE for 15 min and 8 μl of water and 8 μl of 25% glycerol were added to the sample. A 4-μl aliquot of each sample was loaded into separate wells of a 35% poly-

A.

Lane	MPS Disease	Urinary GAG	GalNAc	GlcNAc	IdUA	Gal
2	MPS I	DS/HS	+	+	+	-
3	MPS II	DS/HS	+	+	+	-
4	MPS III	HS	-	+	+	-
5	MPS IV	KS	-	+	-	+
6	Normal	-	-	-	-	-

B.

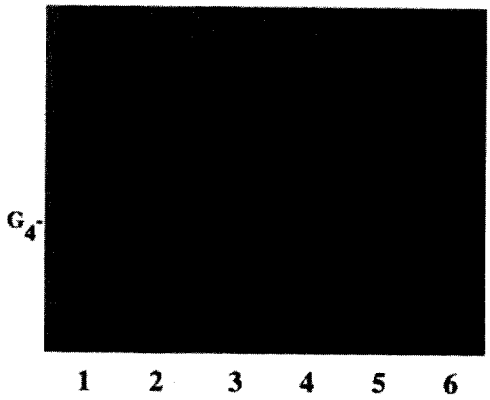

Fig. 8. FACE profiling of glycosaminoglycans. FACE analysis of glycosaminoglycans in patients with different MPS diseases is shown. The GAGs were recovered from 0.5 ml of urine using CPC precipitation following chondroitinase AC digestion. The equivalent of 50 μl of urine was loaded into each lane of the gel. Lane 1 contains the OLIGO Ladder Standard; lane 2 contains the GAGs isolated from patients with MPS I; lane 3, MPS II; lane 4, MPS III; lane 5, MPS IV; and lane 6, normal child. Each MPS disease reveals a different carbohydrate banding pattern due to the presence of different GAGs. Normal urine (lane 6) does not contain significant amounts of GAGs following chondroitinase AC treatment.

acrylamide gel. Electrophoresis was performed at a constant current of 20 mA at 20°C for 1 h.

The different patterns result from each particular lysosomal enzyme defect that causes a different type of GAG to accumulate (Fig. 8A). Fig. 8B shows the fluorophore-labeled GAG–CPC precipitate isolated from a number of different MPS diseases. Since each disease results in the excretion of a different type of GAG, each MPS disease generates a characteristic banding pattern dependent on the type of GAGs excreted in each disease. Due to their size and charge heterogeneity, the GAGs excreted by patients with mucopolysaccharidoses show a broad and complex banding pattern. The same basic methodology described above for MPS disease can be used to identify and analyze GAGs isolated from tissue, as well as GAG chains released from proteoglycans [36].

6. FACE monosaccharide composition analysis

The FACE monosaccharide analysis method described below is another illustration of how changing the type of fluorophore used for derivatization can be used to optimize the separation of carbohydrates in a mixture. The seven common monosaccharides found in the oligosaccharides on glycoproteins have very similar molecular masses. In fact, glucose, mannose, and galactose have identical molecular masses (M_r 180), but are epimers of each other, differing only in the conformation of hydroxyl groups around C-2 and C-4, respectively. In the absence of $-OSO_3^-$ or $-OPO_3H^-$ groups, only the sialic acids are charged. Therefore, the introduction of a charge on neutral monosaccharides is required for electrophoresis. Although separation of ANTS-labeled monosaccharides is possible, and useful for some applications, to take maximal advantage of the structural differences that exist between monosaccharides, we use borate complexation to impart a negative charge for electrophoresis. Borate ions complex with vicinal hydroxyl groups on the monosaccharide [37]. The relative positions of the hydroxyl groups on various monosaccharides, which define the various epimers, determines the relative stability of the borate ion–monosaccharide complex. For this reason, the electrophoresis buffer used for FACE monosaccharide analysis contains borate. It is our belief that the differences in the relative stability of the borate complex, which is dependent on the positions of the hydroxyl group participating in the complex, causes the monosaccharides to migrate to different positions on FACE gels.

6.1. FACE monosaccharide composition analysis of glycoproteins

The monosaccharide composition analysis of a glycoprotein provides useful information on the total amount of carbohydrate or the percentage carbohydrate by weight, as well as the type and ratio of the monosaccharides present in the oligosaccharides [38]. The ability of monosaccharide analysis to quickly reveal changes in the amount of sialic acid makes this type of analysis very useful for evaluating glycoprotein therapeutics, where optimal pharmacokinetics often depends on achieving a high degree of sialylation [39]. Monosaccharide analysis can also be used to provide information relating to the presence of phosphorylated, acetylated, or sulfated sugars, or the presence of other "unusual" types of sugars, e.g. xylose, or N-glycolylneuraminic acid.

FACE monosaccharide composition of human α_1-acid glycoprotein (Sigma, G-9885) was performed and the results are shown in Fig. 9. A total of 30 μg of glycoprotein was divided into three 10-μg aliquots for the separate determinations of neutral and amino sugars, and sialic acids, respectively. Prior to hydrolysis, the glycoprotein was extensively dialyzed against water to remove salts and buffers, and then lyophilized. Neutral monosaccharides were hydrolyzed by dissolving 10 μg in 100 μl of 2 *M* trifluoroacetic acid (TFA) at 100°C for 5 h. N-acetylneuraminic acid (NeuAc) was hydrolyzed by dissolving 10 μg in 100 μl of 0.1 *M* TFA at 80°C for 1 h. Amino sugars were hydrolyzed by dissolving 10 μg in 100 μl of 4 *M* HCl at 100°C for 3 h. Triplicate determinations were made for each type of monosaccharide determination. Following hydrolysis, the reactions were chilled to −20°C and lyophilized in a CVE using the "no heat" setting. The dried monosaccharides from the amino hydrolysis reaction were re-N-acetylated by the addition of 10 μl of re-N-acetylation buffer containing 100 m*M* ammonium carbonate buffer, pH 9.4, and 1 μl of analytical grade acetic anhydride, incubating for 20 min on ice and then re-drying in a CVE.

The dried monosaccharides from each of the three hydrolysis reactions were labeled by adding 2.5 μl of 0.3 *M* 2-aminoacridone (AMAC, see Fig. 1 for structure) in DMSO, 2.5 μl of 30% acetic acid, and 5 μl of 1 *M* $NaBH_3CN$ in DMSO. The labeling reactions were incubated overnight at 37°C and dried in a CVE for approximately 15 min. The labeled samples were resuspended in 5 μl of DMSO, 35 μl of water, and 40 μl of 25% glycerol. A 4-μl aliquot of each reaction was loaded into a lane of a 20% polyacrylamide gel. A standard mixture of monosaccharides consisting of 100 pmol each of AMAC-labeled N-acetylglucosamine (GlcNAc), N-acetylgalactosamine (GalNAc), galactose,

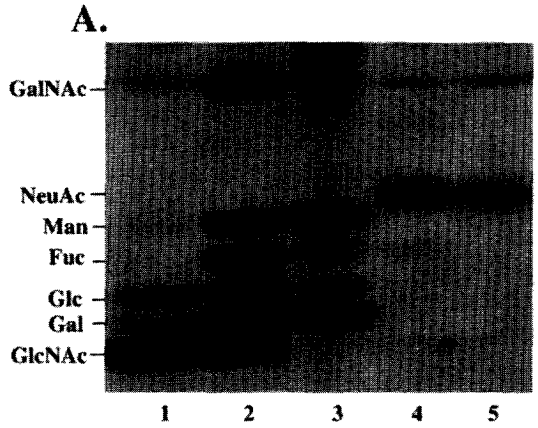

B.

Monosaccharides	FACE mole%	HPLC[40] mole%
GalNAc	0	0
NeuAc	20	19
Man	18	16
Fuc	3	4
Gal	25	21
GlcNAc	34	39

Fig. 9. Monosaccharide composition of human α_1-acid glycoprotein. (A) Lane 1 contains the AMAC-labeled monosaccharides from amino sugar hydrolysis conditions; lane 2, the MONO Ladder Standard 2, monosaccharide identities are indicated on the left of the figure, and the glucose standard band was used for quantification (100 pmol); lane 3, monosaccharides from neutral sugar hydrolysis conditions; lane 4, N-acetylneuraminic acid from sialic acid hydrolysis conditions; and lane 5, the N-acetylneuraminic acid standard (200 pmol). A comparison of the FACE determined mol% with reported values is shown in (B).

mannose, fucose, and glucose was loaded into lanes adjacent to the amine and neutral hydrolysis reactions. For a sialic acid standard, 200 pmol of AMAC-labeled NeuAc was loaded into a lane adjacent to the sialic acid hydrolysis reaction. Electrophoresis was performed at 5°C with a constant current of 30 mA per gel for about 75 min.

Fig. 9 shows the results of the FACE monosaccharide composition analysis of α_1-acid glycoprotein. The existence of specific monosaccharides in the sample is determined by the presence or absence of bands that co-migrates with the corresponding sugar in the standard monosaccharide mix (Fig. 9, lane 2). For example, a band in lane 4 that co-migrates with the NeuAc standard in lane 5 demonstrates that NeuAc is present in the sample. Similarly, the absence of a band in lane 1 that co-migrates with the GalNAc standard in lane 2 demonstrates the absence of GalNAc on α_1-acid glycoprotein. The amount of each monosaccharide in the sample is determined by comparing the intensity of the sample band with the bands in the standard; in this case, each monosaccharide band contains 100 pmol. The percent ratio of the monosaccharides determined by FACE is consistent with reported values as shown in Fig. 9B [40].

6.2. FACE monosaccharide analysis of glycosaminoglycans

Different types of GAGs contain different monosaccharides. Therefore, monosaccharide composition analysis can be an effective method of identifying unknown GAGs isolated from tissue or released from proteoglycans. To illustrate the procedure, Fig. 10 shows the FACE monosaccharide analysis of dermatan sulfate (also called chondroitin sulfate B), keratan sulfate, and heparan sulfate standards obtained from Sigma. These are the types of GAGs found in the urine of children with mucopolysaccharidoses (see Fig. 8A for GAG monosaccharide compositions). In order to obtain an accurate weight, the GAGs were dried for 16 h under P_2O_5. This was performed because GAGs are very hygroscopic and accurate weights can not be

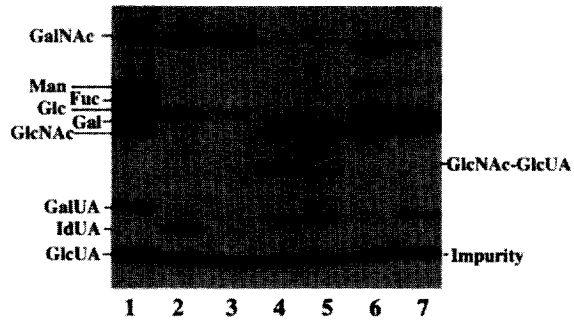

Fig. 10. FACE monosaccharide analysis of glycosaminoglycans. Identification of different types of glycosaminoglycan (GAGs, Sigma) by AMAC labeling of amino sugar hydrolysis products (4 *M* HCl at 100°C for 30 min and 3 h) is shown. Lane 1 contains the GAG Ladder Standard containing 100 pmol of each monosaccharide shown; lane 2 dermatan sulfate, 30 min hydrolysis; lane 3 dermatan sulfate, 3 h hydrolysis; lane 4 heparan sulfate, 30 min hydrolysis; lane 5 heparan sulfate, 3 h hydrolysis; lane 6 keratan sulfate, 30 min hydrolysis; and lane 7 keratan sulfate, 3 h hydrolysis. The 30-min hydrolysis shows the difference between dermatan sulfate, keratan sulfate, and heparan sulfate by the presence of (1) iduronic acid and GalNAc bands for dermatan sulfate, (2) galactose and GlcNAc bands for keratan sulfate, and (3) disaccharide band for heparan sulfate. The 3-h hydrolysis shows the strong GlcNAc band for heparan sulfate.

obtained without extensive drying. A 1-mg/ml stock solution of each type of GAG was prepared in water, and 2.5 μl containing 2.5 μg of each was dried in a CVE. Analysis was performed by hydrolyzing two samples each of the dried glycosaminoglycans in 4 *M* HCl at 100°C for 30 min and 3 h. Following hydrolysis, the reactions were chilled to −20°C and lyophilized. The samples were re-N-acetylated by the addition of 10 μl of re-N-acetylation buffer containing 100 m*M* ammonium carbonate buffer, pH 9.4, and 1 μl of analytical grade acetic anhydride, incubated for 20 min on ice, frozen and lyophilized. To the dried sample was added 5 μl of 0.5 *M* NaH_2PO_4 and the sample was redried. The dried monosaccharides from the six hydrolysis reactions were labeled with AMAC as described for monosaccharide analysis of glycoproteins. The labeled samples were resuspended in 10 μl of DMSO, 30 μl of water, and 40 μl of 25% glycerol. A 4-μl aliquot of each reaction

was loaded into a lane of a 20% polyacrylamide gel. The standard mixture of monosaccharides described above, with the addition of 100 pmol of AMAC-labeled glucuronic acid (GlcUA) and galacturonic acid (GalUA), was loaded into an outside lane of the gel. Electrophoresis was performed at 5°C with a constant current of 30 mA per gel for about 40 min.

Fig. 10 shows that, after hydrolysis, each type of GAG has a different monosaccharide composition profile. In this experiment we hydrolyzed the GAGs for 30 min and 3 h as part of a series of experiments to determine the optimal hydrolysis conditions for each type. In choosing the optimal hydrolysis conditions, one must consider not only the hydrolysis of the bonds joining the monosaccharides together, but also the relative stability of the released monosaccharides in the acid environment. For example, dermatan sulfate shows optimal hydrolysis at 30 min (lane 2), giving GalNAc and iduronic acid. After 3 h the iduronic acid has been degraded (lane 3). On the other hand, heparan sulfate is only partially hydrolyzed in 30 min (lane 4) with some GlcNAcβ1-4GlcUA disaccharide remaining. It is this disaccharide band that can be used to distinguish heparan sulfate from other GlcNAc containing carbohydrates. In 3 h a maximal release of GlcNAc occurs (lane 5), but no or very weak uronic acids are detected, having been degraded during the extended hydrolysis time. Keratan sulfate hydrolysis is maximized at 30 min, revealing both galactose and GlcNAc (lane 6). After 3 h the quantity of galactose has decreased (lane 7) but the amino sugar band is still strong. Chondroitin sulfates A and C also hydrolyze at a slower rate to give a different disaccharide band at 30 min (data not shown). It is interesting to note that keratan sulfate and dermatan sulfate hydrolyze rapidly (usually complete in 30 min), whereas, heparan sulfate and heparin take significantly longer.

6.3. FACE monosaccharide analysis of plant and bacterial polysaccharides

The FACE method can also be used to determine the monosaccharide composition of polysaccharides from plants and bacteria. Plant polysaccharides are usually made up of long polymers of one major type of monosaccharide. For example, Fig. 11 shows the monosaccharide composition of three plant polysaccharides including alginic acid from brown seaweed, wheat starch, and pectin. The monosaccharide analysis procedure involved hydrolysis of the polysaccharide in 4 *M* HCl at 100°C for 1 h, followed by drying, and AMAC labeling as described for monosaccharide analysis of glycoproteins. Pectin contains galacturonic acid (lane 4), wheat starch contains glucose (lane 3), and alginic acid contains mannuronic acid, which forms a lactone under these conditions (lane 2). Although the figure does not contain a standard of mannuronic acid lactone, a commercially available standard was AMAC labeled and found to migrate at the same position as those found in alginic acid (data not shown).

Bacterial polysaccharides contain other types of monosaccharides in addition to those found on glycoproteins, for example, rhamnose, arabinose, xylose, galacturonic acid, glucuronic acid, mannuronic acid, and guluronic acid may be present. Monosaccharide compositional analysis of a bacterial exo-polysaccharide was performed using the same procedure as outlined above for plant polysaccharides, but two hydrolysis reactions were prepared, one for neutral and one for amino sugar analysis. The neutral reaction was not re-N-acetylated (Fig. 11, lane 6) and the amino reaction was re-N-acetylated to detect amino sugars (Fig. 11, lane 7), and standards were loaded into lanes 5 and 8 as indicated. The analysis showed the presence of glucose, and mannose, rhamnose or arabinose which were not mutually resolved in this experiment (lane 6). Weak bands are observed for the amino sugars, GalNAc and GlcNAc (lane 7). For difficult separations such as the mutual separation of mannose, rhamnose, and arabinose, a variety of technical tricks are available that can be used to improve resolution, including the use of different fluorescent dyes to change mobility patterns. For example, ANTS can be used to separate rhamnose, arabinose, and mannose from each other on a 35% polyacrylamide

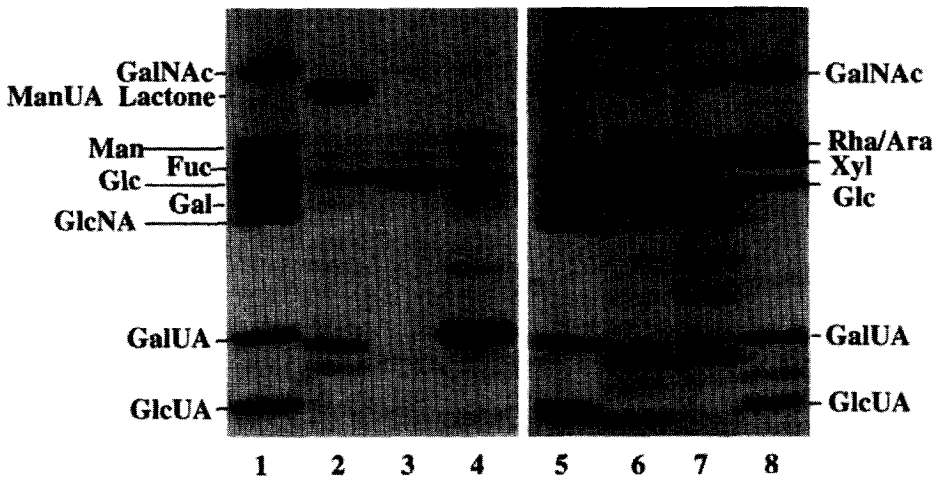

Fig. 11. Monosaccharide composition of various plant and bacterial polysaccharides. Lane 1 contains the GAG Ladder Standard; lane 2 contains 1-h amino sugar hydrolysates of alginic acid, a major matrix polysaccharide in brown seaweed; lane 3 contains wheat starch, and lane 4 contains pectin. Hydrolysis of alginic acid gives mannuronic acid and mannuronic acid lactone; hydrolysis of wheat starch gives glucose, and hydrolysis of pectin gives galacturonic acid. Hydrolysates of bacterial polysaccharides are shown in lanes 6 and 7. Lane 6 shows the hydrolysis products of bacterial exo-polysaccharide optimized for neutral sugars and lane 7 contains the same reaction re-N-acetylated for amino sugar identification. Lanes 5 and 8 contain standards as indicated.

gel. Using the ANTS method we did not find arabinose in this sample, but did find mannose and rhamnose (data not shown).

7. FACE oligosaccharide sequencing

Although oligosaccharide profiling and monosaccharide analysis provide a great deal of information regarding the amount and general nature of the carbohydrates in a sample, many projects require a detailed analysis of one or more oligosaccharide. FACE oligosaccharide sequencing (shown schematically in Fig. 4) is based on the use of exo-glycosidases to specifically degrade the oligosaccharide by removing individual types of monosaccharides from the non-reducing end. This degradation is performed in a stepwise fashion, using mixtures of exo-glycosidases, so that intermediate structures can be identified. The procedure begins with the isolation of a single oligosaccharide band or band region (containing co-migrating oligosaccharides) from a profiling gel. Oligosaccharide purification from a profiling gel is readily performed by using a razor blade to cut out the region containing the ANTS labeled oligosaccharides and eluting the oligosaccharides into water. When excising the bands, it is not necessary to be overly concerned about band contamination because, as we will show, FACE can be used to sequence individual oligosaccharides present in oligosaccharide mixtures. Once the oligosaccharides are recovered from the gel, they are dried and aliquoted into tubes for sequencing.

7.1. Oligosaccharide band preparation for sequencing

To perform FACE sequencing of oligosaccharides, the fluorophore-labeled oligosaccharides are first separated on a profiling gel as described above. Depending on the amount of oligosaccharides present (approximately 300 pmol is required for sequencing), a preparative gel containing multiple lanes of the labeled profiling mixture may need to be prepared. At the completion of electrophoresis, the gel cassette is opened and the gel is placed on a long-wave UV light box (368 nm is recommended). The oligo-

saccharide band(s) that are to be sequenced are excised from one or more lanes, and the slice of acrylamide is placed in 0.5 ml water for 16 h at 4°C. The labeled oligosaccharides are small and charged so they will elute rapidly from the gel into the water. After the incubation in water, the water is recovered from the gel slice and it is dried in a CVE.

7.2. FACE sequencing of N-linked oligosaccharides from glycoproteins

For sequencing of N-linked oligosaccharides the eluted and dried oligosaccharide bands, following the gel isolation described above, are resuspended in 20 μl of water, and equal aliquots are divided into five tubes (see Fig. 4 for overall sequencing strategy). To each tube, 2 μl of one or more of the following enzymes is added according to the matrix shown in Fig. 4: α-fucosidase (Glyko; FUCase I), α-mannosidase (Glyko; MANase II), neuraminidase (Glyko; NANase III), β-galactosidase (Glyko; GALase I), and β-N-acetylhexosaminidase (Glyko; HEXase III). For example, tube 2 received just NANase III, but tube 5 receives 2 μl of each of the five enzymes. The first of the five tubes serves as an undigested control, and receives no enzyme. The reactions are incubated overnight (16 h) at 37°C. The reactions are dried in a CVE and resuspended in 4 μl of water. A 2-μl aliquot from each enzyme digest is mixed with 2 μl of 25% glycerol and loaded into separate lanes of an oligosaccharide profiling gel in the sequence illustrated in Fig. 4. The undigested control, an oligosaccharide ladder standard (Glyko), and a mixture of labeled Manβ1-4GlcNAcβ1-4GlcNAc and Manβ1 – 4GlcNAc[Fucα1–6]β1–4GlcNAc (Glyko) are applied to the gel as standards. Electrophoresis is performed as described for N-linked oligosaccharide profiling. The positions of specific oligosaccharides relative to the bands in the wheat starch ladder, as well as the shifts in migration distances resulting from exo-glycosidase digestions are greatly influenced by the percentage of acrylamide in the gel [28]. Therefore, it is essential that the sequencing analysis of N-linked oligosaccharides, as described below, be performed on 21% polyacrylamide gels, so that the oligosaccharide positions conform to the positions listed in Table 1 and the mobility-shift rules used for sequence analysis presented in Fig. 12B.

The FACE sequencing of an N-linked oligosaccharide band isolated from the mixture is shown in Fig. 12A, the starting mixture of oligosaccharides is in lane 2. The position of the isolated upper band from lane 2 is shown in lane 3, and the bands of the enzymatically degraded oligosaccharides are shown in lanes 4–7. The upward shift created by digestion with neuraminidase, between lanes 3 and 4, reveals that the isolated oligosaccharide contains sialic acid. The degree of shift relative to the bands in the glucose ladder in lane 1, shows an upward shift of 1.5 DP unit, from DP = 7.5 in lane 3 to DP = 9.0 in lane 4, which indicates that one sialic acid was released. The same type of analysis, that is, the determination of migration shifts of bands between adjacent lanes, is continued across the entire gel. The band positions and DP shifts resulting from the continued enzymatic degradation of the oligosaccharide reveals that the starting oligosaccharide is a biantennary oligosaccharide with one sialic acid and one galactose at the non-reducing end of each branch. Similar sequencing experiments with standard oligosaccharides were performed to develop a series of migration rules governing the mobility shifts that are observed as each type of monosaccharide is released. These rules are shown in Fig. 12B and can be used to determine the number of sugar residues released corresponding to the mobility shifts observed between adjacent lanes.

As anyone performing routine oligosaccharide sequencing can attest, one of the greatest challenges using alternative sequencing methods is obtaining sufficient oligosaccharide purity (>95% purity is generally required). Using alternative methods, if fractions contain oligosaccharide mixtures, then overlapping sequences will be obtained, making interpretation of the data very difficult, if not impossible. As shown in Fig. 13, FACE oligosaccharide sequencing is not restricted to highly purified oligosaccharide

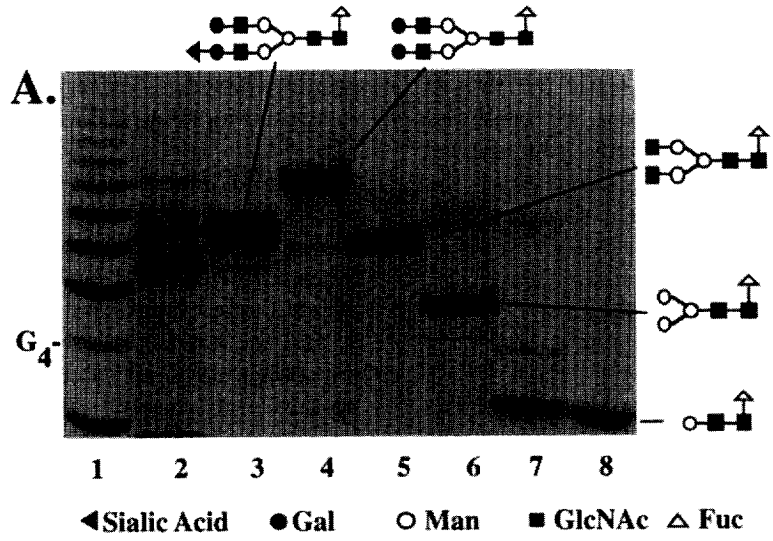

B.

Rules for Predicting Monosaccharide Composition Based on Mobility Shifts	
NeuAc	decreases by average of 1.0 DP
Gal	increases by 1.0 DP
GlcNAc	increases by 0.75 DP
Man	increases by 0.75 DP
Fuc	increases by 0.50 DP
bisecting GlcNAc	increases by 0.50 DP

Fig. 12. Sequence analysis of N-linked oligosaccharides released from a glycoprotein. (A) Lane 2 shows the profile of N-linked oligosaccharides released from a glycoprotein. This profile shows two distinct bands. The upper band was isolated from the gel by soaking the excised acrylamide strip containing the band in water overnight. The recovered band is shown in lane 3. The sequence strategy described in Fig. 3 was used to identify the sequence of the isolated band in lane 3. Based on the DP positions of the bands after digestion (neuraminidase digestion product in lane 4, neuraminidase plus β-galactosidase in lane 5, etc.), and using the sequencing rules based on DP shifts after the loss of a monosaccharide shown in (B), the isolated band in lane 3 was determined to be a monosialylated, biantennary oligosaccharide with core fucose.

bands. Because FACE sequencing is performed by setting up individual enzymatic digestions and these digests are analyzed in adjacent lanes, the sequences of individual oligosaccharides present in mixtures can often be determined with a high degree of confidence. For example, Fig. 13 shows the sequencing of an oligosaccharide band (lane 3) isolated from a mixture of N-linked oligosaccharides (lane 2 shows the profile of the mixture) released from a glycoprotein. Clearly, this isolated band contains at least two oligosaccharides, as revealed by the presence of a doublet in lane 3. Digestion of these isolated oligosaccharides with neuraminidase (digestion product shown in lane 4) shows the characteristic upward band mobility shift due to loss of the negatively charged sialic acid. This digestion reveals that the starting band contained not two, but three different oligosaccharides (three distinct bands in lane 4). Only two of the bands

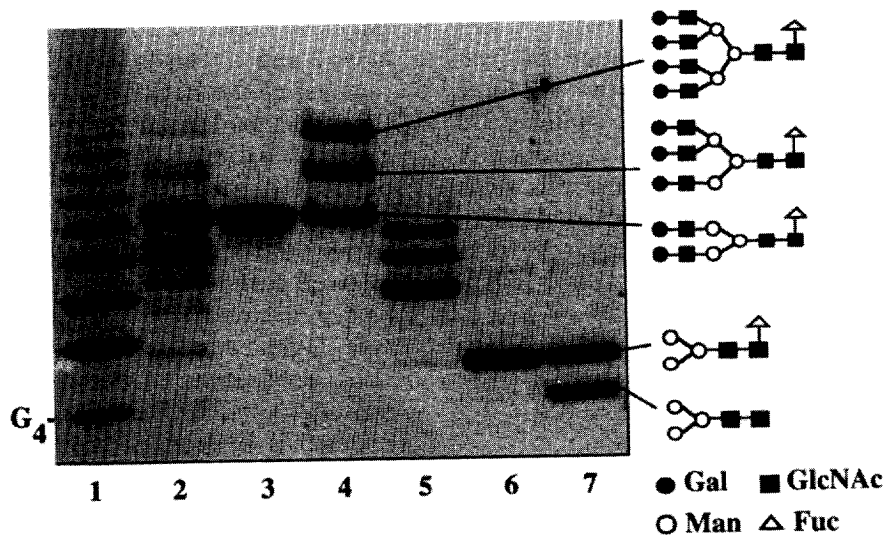

Fig. 13. Sequence analysis of an oligosaccharide mixture. The sequencing strategy described in Fig. 3 was used. Using the sequencing rules based on DP shifts after the loss of a monosaccharide (Fig. 12B), and using the band quantification to aid in tracking the shifts of individual bands between adjacent lanes, the sequence of the three co-migrating oligosaccharides was determined to be (1) asialo galactosylated biantennary with core fucose, (2) monosialylated triantennary with core fucose, and (3) disialylated tetraantennary with core fucose. Standards are shown in lane 7.

shifted from the original starting position, indicating that only two of the oligosaccharides in the band contain sialic acid. Digestion of the starting material with neuraminidase plus β-galactosidase (lane 5) caused a downward shift of all three bands relative to their position in lane 4. The amount of shift between these adjacent lanes indicates a loss of four galactose residues from the upper band, three from the middle band, and two from the lower band. Further digestion with these two enzymes plus β-N-acetylhexosaminidase results in only one band (lane 6), which co-migrates with the fucosylated trimannosyl chitobiose core of the standard in lane 7. This confirms the presence of fucose on the core chitobiose of all of the oligosaccharides. The oligosaccharide structures shown in Fig. 13 were assigned based on a knowledge of the general structural features of N-linked oligosaccharides, the pre-determined migration patterns of oligosaccharides of known sequence (Table 1), and the degradation patterns resulting from digests with the exo-glycosidases based on the mobility shift rules shown in Fig. 12B. Therefore, for the three oligosaccharides in the isolated band (lane 3), there is no sialic acid on the biantennary, core fucosylated oligosaccharide (lowest band in lane 4); one sialic acid on the triantennary, core fucosylated oligosaccharide (middle band in lane 4); and two sialic acids on the tetraantennary, core fucosylated oligosaccharide (highest band in lane 4).

Because the fluorophore remains on the reducing end during sequencing, individual bands can be tracked through the sequencing reaction by determining the number of picomoles in each band. Each carbohydrate band can be followed through the entire sequencing reaction, lane by lane, independent of the others in the mixture. For example, the three bands in lane 4 contain, from top down, 68, 93, and 178 pmol, respectively. The three bands in lane 5 contain from top down 64, 86, and 166 pmol, respectively. By tracking the bands in adjacent lanes containing the same number of pmol, we see that the upper band in lane 4 moved down the gel a total of 4 DP units to the position of the upper band in lane 5, the middle band in lane 3 moved to the middle position of lane 5, and the lower band in lane 4 moved to the lowest band position in lane

5. In lane 6, after the terminal GlcNAc residues have been removed by the addition of hexosaminidase to the enzyme mixture, all three bands migrate together in a band containing 352 pmol (total of all three bands) at the position of the $Man_3GlcNAc[Fuc]GlcNAc$ standard, which is shown in lane 7. Tracking individual oligosaccharide bands in sequencing mixtures works best when the relative amount of each oligosaccharide differs by greater than 5%.

7.3. FACE sequencing of O-linked oligosaccharides from glycoproteins

Serine- and threonine-linked oligosaccharides can also be sequenced using a variation in the types of glycosidases included in each reaction. Although the overall sequencing strategy for O-linked oligosaccharides is similar to that described above for N-linked oligosaccharides, the migration shift rules for sialic acid release are different. For example, when the sialic acid residues on an N-linked type oligosaccharide are removed using neuraminidase, the location of the remaining asialo-oligosaccharide is higher in the gel (reduced mobility) relative to the sialylated oligosaccharide, as shown in Fig. 12A, lanes 3 and 4. This is thought to result from the removal of the negative charges contributed by the sialic acid residues, resulting in a lower charge/mass ratio. The DP shift in the positions of the two bands, relative to the bands in the wheat starch ladder (lane 1), is used to determine the number of NeuAc residues that were released during the digestion (Fig. 12B). As will be demonstrated below, when sequencing mucin-type O-linked oligosaccharides, the release of sialic acid results in a downward shift (faster migration) and the number of sialic acid residues released is determined using a partial digestion with neuraminidase. The reversal of mobility shift rules for sialic acid probably results from mucin-type oligosaccharides being generally smaller than N-linked oligosaccharides, thus requiring the use of higher percentage gels for optimal band separations for O-linked oligosaccharide analysis (35% versus 21% for N-linked oligosaccharide analysis), resulting in greater sieving by the gel matrix during electrophoresis.

An example of the mobility shifts resulting from exo-glycosidase digestions of O-linked mucin-type oligosaccharides is shown in Fig. 14.

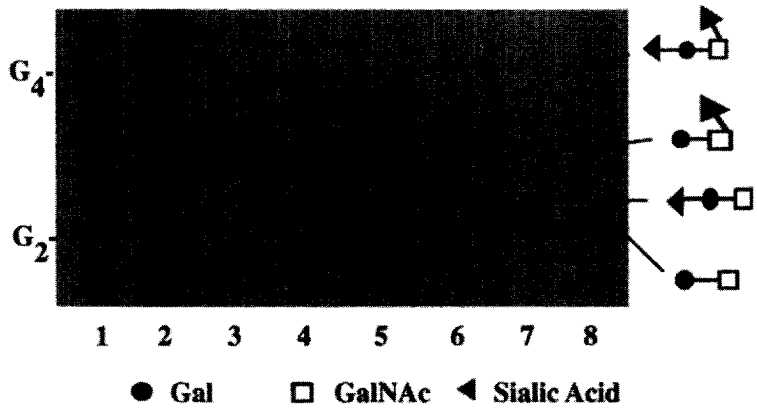

Fig. 14. Sequence analysis of O-linked oligosaccharides from bovine fetuin. Lane 1 contains the OLIGO Ladder Standard; lane 2, the profile of O-linked released oligosaccharides; lane 3, the isolated band 1; lane 4, partial digestion of the isolated band 1 with NANase III (Glyko); lane 5, complete digestion with NANase III; lane 6, isolated band 2; lane 7, digestion of isolated band 2 with NANase III; and lane 8 contains standard Galβ1–3GalNAc. The first oligosaccharide contained two sialic acid residues and the second oligosaccharide contained only one sialic acid. Both isolated bands migrate consistent with Galβ1–3GalNAc after complete NANase III digestion. Bovine fetuin contains both a tetrasaccharide with two sialic acids, a Galβ1–3GalNAc core, and a trisaccharide with a single sialic acid and Galβ1–3GalNAc core.

Fetuin contains three mucin-type O-linked oligosaccharides consisting of a monosialylated trisaccharide, a disialylated tetrasaccharide, and a disialylated hexasaccharide, all of which contain a Galβ1–3GalNAc core at the protein attachment site [41]. The O-linked oligosaccharides were released from fetuin using a hydrazine-based, O-linked oligosaccharide release kit (Glyko), and three oligosaccharides were detected. Fig. 14, lane 2 contains the three O-linked oligosaccharides attached to bovine fetuin. The two lower bands were isolated from the gel as described above and sequenced. Lane 4 shows a partial digest of the isolated intermediate band at DP = 2.9 (lane 3), using neuraminidase. This digest resulted in three bands (lane 4). The top band is the undigested oligosaccharide, the middle band represents the removal of one sialic acid residue. The bottom band represents the removal of a different sialic acid residue and the band resulting from the complete digestion (lane 5) co-migrates with the Galβ1–3GalNAc standard, which was loaded into lane 8. Further analysis of this oligosaccharide using linkage-specific neuraminidases revealed that the intermediate band in lane 4 was Gal[NeuAc(α2–6)]GalNAc, and the lower band was NeuAc(α2–3)Galβ1–3GalNAc (data not shown). Therefore, the isolated band in lane 3 at DP = 2.9 is the O-linked tetrasaccharide containing two NeuAc residues, one linked α2–3 to galactose and the second linked α2–6 to GalNAc, which is consistent with the analysis by Edge and Spiro [41]. The lower band in the profile in lane 2 at DP = 2.4 was also isolated (isolated band shown in lane 6), and digested with an α2–3 specific neuraminidase (NANase I, Glyko) (digestion product shown in lane 7). The digestion product showed a downward shift following neuraminidase digestion, and the remaining oligosaccharide co-migrated with the Galβ1–3GalNAc standard (lane 8). We therefore identified this oligosaccharide as the trisaccharide containing one NeuAc residue linked α2–3 to the galactose. Although it has not been sequenced, we believe that the faint upper band in lane 2 at approximately DP = 4.4 is the disialylated hexasaccharide of fetuin.

8. Enzyme-based disaccharide analysis of glycosaminoglycans

Glycosaminoglycans are composed of repeating disaccharide units containing one amino sugar and one uronic acid. Glycosaminoglycans are charged because the sugars contain $-SO_3^-$ groups at various positions, either as N or O sulfoesters. The variation in the location of the $-SO_3^-$ groups creates a degree of heterogeneity along an otherwise homogeneous polymer chain. Determining the positions of $-SO_3^-$ groups on the disaccharides is important because this often defines sites of protein binding along the GAG chain. Determining positions of $-SO_3^-$ groups along the chain and the relative amounts of disaccharides with specific $-SO_3^-$ configurations can be performed using FACE either chemically, using nitrous acid, or enzymatically, using specific endo-glycosidases [36].

Fig. 15 illustrates how endo-glycosidases can be used to determine the disaccharide composi-

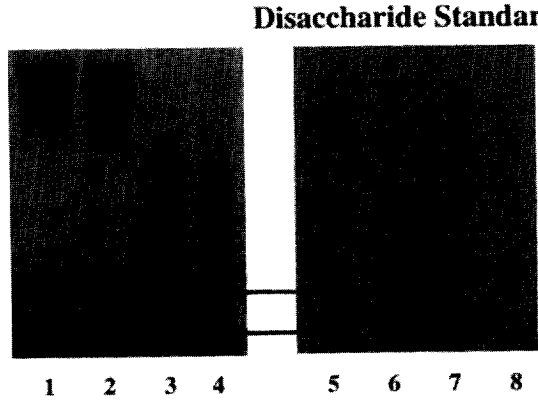

Fig. 15. Profiles of the heparinase I digested bovine lung heparin. Lane 1 contains undigested heparin; lane 2, partial digestion of heparin with heparinase; lane 3, further digestion with heparinase; lane 4, 30-min digestion with heparinase. Further digestion with heparinase did not result in further degradation of this preparation of heparin. Only through the combined use of heparinase I and II was complete degradation to disaccharides achieved. The disaccharide standards (lanes 5–8) are: αΔUA2S(β1–4)GlcNS6S (IS), αΔUA(β1–4)GlcNS6S (IIS), αΔUA2S(β1–4)GlcNS (IIIS), and αΔUA(β1–4)GlcNS (IVS), all obtained from Sigma. The major disaccharides obtained by digestion of bovine heparin are IS and IIIS.

tion of bovine lung heparin. The profile of bovine lung heparin is shown in lane 1 of Fig. 15. An amount of 2 μg of heparin was digested with 1000 mU of heparinase I (Glyko) for 1 min (lane 2), 5 min (lane 3), and 10 min (lane 4) at 37°C. The digests were dried in a CVE and then resuspended in 5 μl of ANTS, 0.15 *M* in 15% acetic acid and 5 μl of 1 *M* $NaBH_3CN$ in DMSO. The labeling mixture was incubated for 16 h at 37°C. The samples were dried and re-suspended in 20 μl of water. Then 2 μl of the re-suspended material was combined with 2 μl of 30% glycerol. The entire 4-μl sample was loaded into a single lane of a 35% polyacrylamide slab gel and the gel was run at 15 mA constant current for 1–2 h at 20°C. Disaccharide standards (Sigma) are shown in lanes 5–8 in Fig. 15 and their structure are shown in the figure legend.

The results of the heparinase I digestion reveal that bovine heparin contains the IS disaccharide and the IIIS disaccharide. Bands above the IS disaccharide band in lane 4 are probably tetrasaccharides that are resistant to heparinase I digestion. Heparinase I requires an N-sulfated ($-NSO_3^-$) ester on the C-2 amine of $GlcNH_2$ and an O-sulfated ($-OSO_3^-$) ester on the C-2 position of the adjacent iduronic acid residue. If these positions are not sulfated, then the enzyme will not cut and a tetrasaccharide or longer polymer results. Sequential digestions of heparin with heparinase I, followed by heparinase II (Sigma), which does not require the presence of the $-OSO_3^-$ ester on the C-2 position of iduronic acid, resulted in complete digestion of the heparin into disaccharides.

9. Enzymatic detection of modified carbohydrates

In the examples shown above, the choice and sequence of addition of exo-glycosidases used for sequencing takes full advantage of the oligosaccharide sequences that are usually encountered in different classes of oligosaccharides, the canonical core structures for N- and O-linked oligosaccharides, and the usual types of branching points and linkage configurations. These sequence predictions are based on our current understanding of the N-linked and O-linked oligosaccharide synthetic pathway and the oligosaccharide sequence data that has accumulated over the years. These expectations suggest the types and order of enzymes that are used for sequencing. Indeed, much of the time oligosaccharide sequences fit the expected patterns, but some may not. As discussed above, oligosaccharides can be modified with $-PO_4^-$, $-SO_4^-$ groups, and may contain unexpected types of monosaccharides as well as unusual linkages and branch points.

These modifications are essentially impossible to detect using traditional oligosaccharide profiling or mapping techniques. These modification on oligosaccharides can be detected by monitoring gel shifts (or the absence of gel shifts) following exo-glycosidase digestions. Glycosidases are highly specific enzymes with respect to the type of monosaccharide they remove, its anomericity, and sometimes the penultimate sugar linkage, as well as the presence of substitutions. Therefore, any encountered resistance of a given oligosaccharide band to sequential exo-enzyme digestion suggests the presence of unexpected linkages or modifications. One example of the detection of sugar modifications by resistance to glycosidase digestion is shown in Fig. 16. When the oligosaccharides released from a glycoprotein were sequenced according to the procedure outlined in Fig. 4, we found that a number of the oligosaccharides were resistant to α-mannosidase digestion (data not shown). These results suggested that the internal mannose residues of these oligosaccharides might be modified with $-PO_4H^-$ groups, making then resistant to α-mannosidase cleavage. To test this idea, we digested the mixture of oligosaccharides with alkaline phosphatase, which releases $-PO_4H^-$ groups from carbohydrates, followed by neuraminidase, and compared the mobility of the resulting oligosaccharides to the mobility of the oligosaccharides digested with neuraminidase alone (Fig. 16). The alkaline phosphatase plus neuraminidase treated oligosaccharides caused an upward shift in band positions (Fig. 16, lane

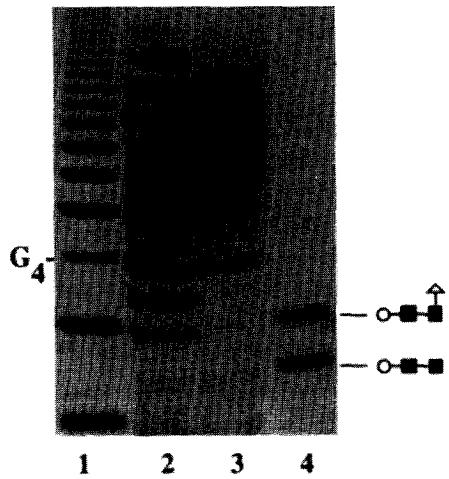

Fig. 16. Detection of phosphorylated oligosaccharides. Digestion of rPNGase F (Glyko) released oligosaccharides from a recombinant glycoprotein was performed using alkaline phosphatase from calf intestine (Boehringer Mannheim Cat No. 713-023). Lane 1 contains the OLIGO Ladder Standard; lane 2, the NANase III digested oligosaccharides; lane 3, the NANase III digested oligosaccharides after treatment with alkaline phosphatase; lane 4, the core N-linked standards, ManGlcNAc[Fuc]GlcNAc and $ManGlcNAc_2$, as markers. Loss of the lower bands in lane 2 and formation of new bands of slower mobility in lane 3, show loss of phosphate groups. See Fig. 18 for a profile showing non-phosphorylated oligosaccharides treated with alkaline phosphatase.

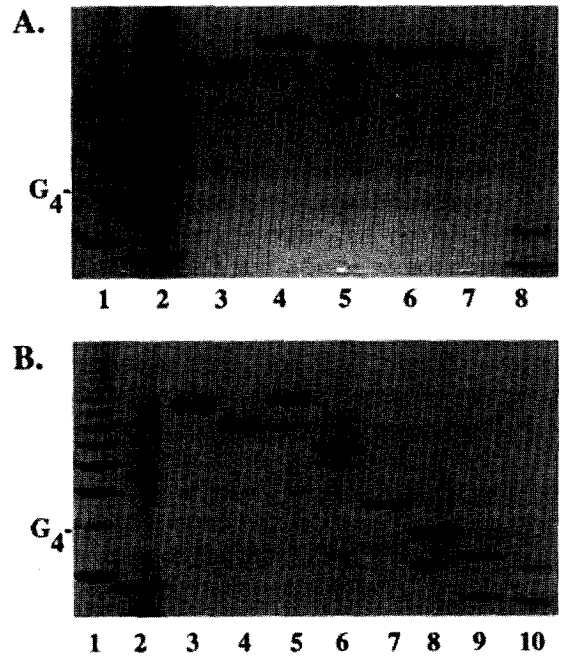

Fig. 17. Sequence analysis of an oligosaccharide containing α-linked galactose. Sequencing of an ANTS-labeled isolated band from a recombinant mouse cell line glycoprotein is shown. (A) represents the image obtained using the sequence strategy described in Fig. 3. Digestion of the band stops short of an expected N-linked core oligosaccharide. (B) shows use of a modified sequence strategy. Treating the isolated band with α-galactosidase first (lane 4 in B) and the addition of α-galactosidase to each of the regular sequence reactions, allows digestion of the band to the fucosylated core. Only partial digestion is observed with α-mannosidase. Digestion with α-fucosidase in lane 9 shows that the sample did indeed contain core fucose.

3) relative to the positions of the oligosaccharides digested with neuraminidase alone (Fig. 16, lane 2). Not all of the oligosaccharide bands shifted up in the gel, suggesting that some of the oligosaccharides do not contain $-PO_4H^-$. The oligosaccharides shifted up because of the removal of the negative charge contributed by the $-PO_4H^-$ residue. This showed that the mannose residues on the oligosaccharides contain phosphate. A repeat of the original sequencing reaction, but with the addition of alkaline phosphatase to the reaction tubes, enabled the reaction to go to completion (data not shown).

An example of the detection of an unexpected monosaccharide linkage by resistance to glycosidase digestion is shown in Fig. 17. Fig. 17A shows the sequencing of an oligosaccharide isolated from the mixture in lane 2 according to the sequencing strategy outlined in Fig. 4. The purified undigested oligosaccharide is shown in lane 3. The enzymatic digests shown in lanes 4–7 were performed as described above and as illustrated in Fig. 4. Digestion with neuraminidase gave readily interpretable results of an upward shift of 1.5 DP units relative to the ladder in lane 1, indicating the release of at least one sialic acid residue. However, the shift of the digestion product between lanes 4, 5 and 6 was unexpected, in that the degree of shift indicated that only one galactose was released in lane 5 (one DP shift between lanes 4 and 5), and only one GlcNAc residue was released in lane 6 (0.75 DP

shift between lanes 5 and 6). These results suggested that the galactose residues were either modified in some way or attached to the penultimate GlcNAc through an unexpected linkage. Since this sample was a recombinant glycoprotein expressed in mouse cells, we suspected that the oligosaccharides might contain alpha-linked galactose, which has been found on glycoproteins expressed in mouse cell lines [42]. Therefore, we repeated the sequencing experiment as before, but with the addition of α-galactosidase in each reaction, and this second sequencing experiment is shown in Fig. 17B. This second sequencing experiment was performed as follows. First, the starting oligosaccharide (Fig. 17B, lane 3) was digested with α-galactosidase alone (lane 4). The oligosaccharide shifted down in position two DP units, which is consistent with the release of two alpha-linked galactose residues. Further digestion with neuraminidase (α2–3 linkage specific, NANase I, Glyko) plus α-galactosidase resulted in the loss of one sialic acid residue (lane 5), which was consistent with our previous results (Fig. 17A). Continued digestion with α-galactosidase in addition to the enzymes listed in Fig. 4 resulted in the release of three galactose residues (lane 6), followed by a normal sequencing pattern for a triantennary oligosaccharide terminating with three GlcNAc residues with core fucose. The conclusion from these experiments is that this triantennary oligosaccharide contains Gal(α1–3)Gal(β1–4)-GlcNAc at the non-reducing terminus of two branches and the third branch contains sialic acid(α2–3)Gal(β1–4)GlcNAc.

10. FACE glycosylation "fingerprinting"

The ability of FACE to sequence mixtures of oligosaccharides can be further extended by digesting the entire population of oligosaccharides released from a glycoprotein. This procedure can quickly reveal a great deal of structural information about the oligosaccharides in the mixture. For example, starting with 10 μg of a glycoprotein containing ca. 50% carbohydrate, we were able to obtain information on (1) the types of oligosaccharide present (complex, high-mannose, hybrid), (2) the types of branching present, and (3) whether the oligosaccharides are phosphorylated, sialylated or fucosylated. Using the sequence strategy shown in Fig. 4, a portion of the ANTS-labeled mixture of oligosaccharides released from a glycoprotein was digested with exo-glycosidases. Fig. 18A illustrates the results using the N-linked oligosaccharides released from α_1-acid glycoprotein shown in lane 4. Lane 2 contains the mixture of oligosaccharides digested with alkaline phosphatase to detect phosphorylation. Comparison of lane 2 with lane 3, which contains undigested oligosaccharides, shows no change in band mobility, indicating that the oligosaccharides are not phosphorylated. When the starting mixture, shown in lane 3, was digested with exo-glycosidases as illustrated in Fig. 4, a complex degradation pattern emerges across the gel that can be considered a glycosylation "fingerprint" for this protein. Upward shifts of the bands from the starting mixture (lane 3) with neuraminidase digestion indicates the presence of sialic acid in most oligosaccharides (lane 4). The positions of the desialylated parts in lane 4 are consistent with biantennary, triantennary, and tetraantennary branching (Table 1). The fact that multiple bands are present for each type probably indicates differences in branching or ±core fucosylation. The highest bands (DP = 14) suggest the possible presence of polylactosamine structures. Digestion with neuraminidase and β-galactosidase (lane 5) shows multiple bands shifting down, indicating the release of terminal galactose residues. The three lower bands match the DP positions for asialo-, agalacto-biantennary, triantennary and tetraantennary structures (see Table 1). Again, the presence of the upper bands (>DP = 8) suggests branching or polylactosamine structures. Digestion with neuraminidase, β-galactosidase, and β-N-acetylhexosaminidase shows formation of two major bands (lane 6). The lower band is expected and migrates at the same position as the trimannosylchitobiose core at DP = 4.2. The upper band may be due to branching, or a bisecting GlcNAc. Treatment with one more enzyme, α-

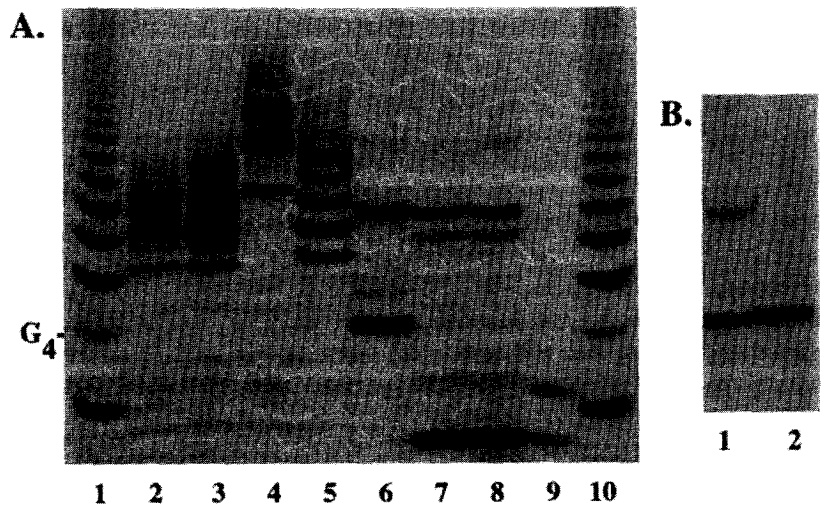

Fig. 18. Glycosylation "fingerprint" of human α-acid glycoprotein. (A) Lane 2 contains the alkaline phosphatase digest of the mixture shown in lane 3. Lane 3 contains the mixture of ANTS-labeled, rPNGase F released, oligosaccharides from α_1-acid glycoprotein. Lanes 4–7 show the digestion of this mixture following the sequence strategy described in Fig. 4. Lane 8 shows the entire mixture of enzymes in lane 7 plus FUCase I, which digests α1-6 fucose linkages. Use of a different α-fucosidase (FUCase II, Glyko) specific for (α1–3,4 linkages (digest shown in B, lane 2) shows the upper band in A, lane 6, which was re-run in B, lane 1 is degraded completely, indicating that at least one fucose is linked β1–3 or 4 to GlcNAc and therefore prevented the β-hexosaminidase digest from going to completion in A.

mannosidase (lane 7), shows the expected mannosylchitobiose core, and at least one mannose residue released from the upper band (lane 7). This means that the upper band in lane 6 contains one undigested GlcNAc branch. When the sample shown in Fig. 18A, lane 6 (also shown in Fig. 18B, lane 1) is digested with an α-fucosidase specific for α1–3,4 linkages, in addition to all other enzymes except α-mannosidase, the upper band collapses to the position of the lower band (Fig. 18B, lane 2). Also note that in lane 8 the α-fucosidase specific for α1–6 linkage shows no digestion of the upper band. Therefore, GlcNAc on the undigested branch, represented by the upper band in lane 6, must be modified by α1–3 or 4 linked fucose.

This glycosylation "fingerprint" indicates that alpha-acid glycoprotein contains carbohydrates of complex type, which are not phosphorylated, but are sialylated, with biantennary, triantennary, and tetraantennary oligosaccharides present. Some of the oligosaccharides also contain fucose linked α1–3,4 to GlcNAc residues on one of the branches, with possibly two fucoses (based on DP position of the uncut band) on the same branch. The oligosaccharides do not contain core fucose.

Although the amount of individual oligosaccharide sequence information obtained using this procedure may be limited due to the complexity of interpreting the band shifts, glycosylation "fingerprinting" is a powerful method for detecting differences in glycosylation between samples. For example, if the degree or type of oligosaccharide changes, or if the oligosaccharides become modified with $-PO_4H^-$, $-SO_3^-$ groups, then the glycosylation "fingerprint" will indicate the presence of these modifications. In a process development or quality control laboratory, this type of analysis will quickly reveal changes that may have occurred due to different cell lines or fermentation conditions used to produce a recombinant glycoprotein. The FACE profiling method allows rapid sample processing and high resolution, while the specificity of the enzymes and their sensitivity to carbohydrate modifica-

tions makes them ideal "probes" for detecting structural changes.

11. Conclusion

In a relatively short time, the FACE method has shown great potential as a flexible and reliable tool for performing routine, as well as, specialized carbohydrate analysis. As we have shown, the main advantages of this method are the sensitivity, the high resolving power of the separation, the ability to use essentially the same protocol for a variety of different applications, and the overall ease of using a familiar medium: slab gel electrophoresis. The ability of the gel system to analyze oligosaccharides without the need for separation of charged and uncharged oligosaccharides simplifies both profiling and sequencing. The slab gel format makes it very easy to compare the positions of oligosaccharides in different samples, as fully exploited in the FACE sequencing strategy. The ability to analyze multiple samples on the same gel makes this an ideal system for performing routine carbohydrate analysis such as often required in process development and quality control laboratories.

Abbreviations

ANTS	Disodium 8-amino-1,3,6-naphthalene trisulfonate
ANDA	Potassium 7-aminonaphthalene-1,3-disulfonate
AMAC	2-Aminoacridone
NeuAc	N-Acetylneuraminic acid
GlcNAc	N-Acetylglucosamine
GalNAc	N-Acetylgalactosamine
GalUA	Galacturonic acid
GlcUA	Glucuronic acid
CCD	Charge-coupled device
FACE	Fluorophore-assisted carbohydrate electrophoresis
HPAEC	High-performance anion-exchange chromatography
HPLC	High-performance liquid chromatography
DP	Degree of polymerization

References

[1] A. Varki, Glycobiology, 3 (1993) 97–130.
[2] M.N. Fukuda, H. Sasaki, L. Lopez and M. Fukuda, Blood, 73 (1989) 84–89.
[3] T. Feizi and R.A. Childs, Biochem. J., 245 (1987) 1–11.
[4] J.C. Paulson, Trends Biochem. Sci., 14 (1989) 272–276.
[5] M.W. Spellman, Anal. Chem., 62 (1990) 1714–1722.
[6] P. Jackson and G.R. Williams, Analysis of Carbohydrates, U.K. Patent Publication No. W088/10422, 1988; P. Jackson, Analysis of Carbohydrates, U.K. Patent Publication No. W091/05256, 1991; P. Jackson, Analysis of Carbohydrates, U.K. Patent Publication No. W092/11531, 1992; P. Jackson, Treatment of Carbohydrates, U.K. Patent Publication No. W091/05265, 1991; P. Jackson, Analysis of Carbohydrates, U.K. Patent Publication No. W093/02356, 1993.
[7] P. Jackson, Anal. Biochem., 216 (1994) 243–252.
[8] P. Jackson and G.R. Williams, Electrophoresis, 12 (1990) 94–96.
[9] P. Jackson, Biochem. Soc. Trans., 21 (1993) 121–125
[10] P. Jackson, Methods Enzymol., 230 (1994) 250–256.
[11] P. Jackson, Electrophoresis, 15 (1994) 896–902.
[12] K.G. Rice, M.K. Rottink and R.J Linhardt, Biochem. J., 244 (1987) 515–522.
[13] K.-B. Lee, A. Al Hakim, D. Loganathan and R.J. Linhardt, Carbohydrate Res., 214 (1991) 155–168.
[14] K.-B. Lee, Y.S. Kim and R.J. Linhardt, Anal. Biochem., 203 (1992) 206–210.
[15] O. Gabriel and G. Ashwell, Trends Glycosci. Glycotechnol., 5 (1993) 225–227.
[16] R.I. Masada, C. Hague, R. Seid, H. Samual, S. McAlister, V. Pigiet and C.M. Starr, Trends Glycosci. Glycotechnol., 7 (1995) 133–147.
[17] W.P. Jencks and J. Carriuolo, J. Am. Chem. Soc., 82 (1960) 1778–1782.
[18] W.P. Jencks, in W.P. Jencks (Editor), Catalysis in Chemistry and Enzymology, McGraw-Hill, Ch. 2, p. 72.
[19] P. Jackson, Biochem. J., 270 (1990) 705–713.
[20] J. March, in J. March (Editor), Advanced Organic Chemistry, Reactions, Mechanisms and Structures, McGraw-Hill, 1977, Ch. 6, p. 819.
[21] R.O. Hutchins, C.A. Milewski and B.E. Maryanoff, J. Am. Chem. Soc., 95 (1973) 3662–3668.
[22] P. Jackson, Anal. Biochem., 196 (1991) 238–244.
[23] K.C. Chan, L.B. Koutny and E.S. Yeung, Anal. Chem., 63 (1991) 746–750.
[24] A.L. Tarentino, C.M. Gómez and T.H. Plummer, Jr., Biochemistry, 24 (1985) 4665–4671.
[25] F. Maley, R.B. Trimble, A.L. Tarentino and T.H. Plummer, Jr., Anal. Biochem., 180 (1989) 195–204.
[26] J. Amano and A. Kobata, Methods Enzymol., 179 (1989) 261–270.
[27] Y.-T. Li and S.-C. Li, Methods Enzymol., 179 (1989) 479–487.
[28] R.J. Stack and M.T. Sullivan, Glycobiology, 2 (1992) 85–92.
[29] G.-F. Hu and B.L. Vallee, Anal. Biochem., 218 (1994) 85–191.

[30] G.-F. Hu, J. Chromatogr. A, 705 (1995) 89–103.
[31] S.S. Basu, S. Dastgheib-Hosseini, G. Hover and Z. Li, Anal. Biochem., 222 (1994) 270–274.
[32] C.M. Starr, J.C. Klock, E. Skop, I. Masada and T. Giudici, Glycosylation Disease, 1 (1994) 165–176.
[33] J.C. Klock, C.M. Satarr, D.J. Pyrce, E. Skop and P. Edridge, Int. J. Pediatr., 9 (1994) 1–9.
[34] E. Wessler, Anal. Biochem., 26 (1967) 439–444.
[35] M.W. Teller and A. Ziemann, Hormone Metab. Res., 1 (1969) 32–35.
[36] T.A. McCaffery, S. Consigli, D. Baoheng, D. Falcone, A. Mazid and C.M. Starr, (1995) submitted for publication.
[37] S. Hoffstetter-Kuhn, A. Paulas, E. Gassmann and H.M. Widmer, Anal. Chem., 63 (1991) 1541–1547.
[38] D.L. Blithe, Endocrinology, 126 (1990) 2788–2798.
[39] M. Takeuchi and A. Kobata, Glycobiology, 1 (1991) 337–346.
[40] I. Yamashina, Acta Chem. Scand., 10 (1956) 1066–1072.
[41] A.S.B. Edge and R.G. Spiro, J. Biol. Chem., 262 (1987) 16135–16141.
[42] C.A.K. Borrebaeck, A.-C. Malmborg and M. Ohlin, Immunol. Today, 14 (1993) 477–479.